Disease modification upon brief exposure to tofacitinib during chronic epilepsy.

Olivia R. Hoffman[1,2], Jennifer L. Koehler[1,2], Jose Ezekiel Clemente Espina[1,3], Anna M. Patterson[1], Emily S. Gohar[1], Emanuel Coleman[4], Barry A. Schoenike[1], Claudia Espinosa-Garcia[5], Felipe Paredes[5], Raymond J. Dingledine[5], Jamie L. Maguire[4], Avtar S. Roopra[1,2,3]*

[1]Department of Neuroscience, University of Wisconsin-Madison School of Medicine and Public Health, Madison, WI 53705, USA; [2]Molecular and Cellular Pharmacology Graduate Program, University of Wisconsin-Madison School of Medicine and Public Health, Madison, WI 53705, USA; [3]Cellular and Molecular Biology Graduate Program, University of Wisconsin-Madison School of Medicine and Public Health, Madison, WI 53705, USA; [4]Department of Neuroscience, Tufts University School of Medicine, Boston, MA 02111, USA; [5]Department of Pharmacology & Chemical Biology, Emory University School of Medicine, Atlanta, GA 30322, USA.

* asroopra@wisc.edu

ABSTRACT

All current drug treatments for epilepsy, a neurological disorder affecting over 50 million people[1,2] merely treat symptoms, and a third of patients do not respond to medication. There are no disease modifying treatments that may be administered briefly to patients to enduringly eliminate spontaneous seizures and reverse cognitive deficits[3,4]. Applying network and systems-based approaches to rodent models and human temporal lobectomy samples, we observe the well-characterized pattern of rapid induction and subsequent quenching exhibited by the JAK/STAT pathway within days of epileptic insult. This is followed by an utterly unexpected, resurgent activation months later with the onset of spontaneous seizures. Targeting the first wave of activation after epileptic insult does not prevent disease. However, brief inhibition of the second wave with CP690550 (Tofacitinib)[5,6] enduringly suppresses seizures, rescues deficits in spatial memory, and restores neuropathological alterations to naïve levels. Seizure suppression lasts for at least 2 months after last dose. Using discovery-based transcriptomic analysis across models of epilepsy and validation of putative mechanisms with human data, we demonstrate a powerful approach to identifying disease modifying targets; this may be useful for other neurodegenerative diseases. With this approach, we find that reignition of inflammatory JAK/STAT3 signaling in chronic epilepsy opens a powerful window for disease modification with the FDA-approved, orally available drug CP690550.

INTRODUCTION

Epilepsy is a highly prevalent neurological disorder with over 50 million cases worldwide[1,2]. Arising from a myriad of etiologies including gene mutations and environmental insults, the unifying characteristic of the epilepsies is the emergence of spontaneous, recurrent seizures (SRS). Anticonvulsants aimed at controlling seizures are the current first-line treatments for epilepsy. No current treatments have been shown to prevent, let alone reverse, disease progression. Patients often remain on medication for life, as no treatments are disease modifying[3]. Further, despite the introduction of 12 new antiseizure drugs in the last 20 years, 30% of patients are drug resistant, a rate that has remained constant since 1850[4,5]. Finally, with few exceptions[6,7], long-term use of many anti-epileptic drugs is associated with a marked decline in cognition[8], highlighting the need for transient treatments with enduring effects that address the mechanisms underlying disease mechanisms, not just seizures.

In acquired epilepsies, epileptogenesis is the process that links the eventual propagation of spontaneous seizures to an acute, initiating traumatic insult[9-11]. Status epilepticus (SE), a severe bout of unremitting seizures, is one of the most common methods for modeling epileptogenesis in acquired epilepsies. This process is associated with a number of changes in the brain including molecular, cellular, and network alterations in plasticity and inflammation[12]. Many signaling cascades exhibit a transient period of explosive activation that abates within days. How these cascades react to the onset of spontaneous seizures in chronic epilepsy is poorly characterized, and it is not known whether mechanisms invoked early after insult are reengaged upon disease establishment.

Antiepileptogenic therapies aim to prevent progression to spontaneous seizures through early intervention, although the lack of biomarkers for epilepsy makes this approach challenging in clinical practice. Disease

modifying therapy would aim to slow or reverse the progression of chronic epilepsy after spontaneous seizures are manifest. Currently, there are no FDA approved therapeutic interventions that modify disease in an enduring manner upon brief administration[3].

Of the studies that have profiled gene changes in the epileptic brain, nearly all observe robust activation of inflammatory pathways that is quenched within days of SE[13-19]. In the brain, inflammation can be triggered by glial cells[20] as well as neurons[21]. Others have used anti-inflammatory drugs with varying degrees of success to suppress seizures in human patients[22-25], and some drugs targeting neuroinflammation in rodents have shown antiepileptogenic potential[26-29]. However, the endogenous mechanisms that regulate neuroinflammation post-SE – acutely and chronically – are poorly understood. Recently, we applied a systems approach to a transcriptomic consortium dataset that incorporated gene expression data across multiple laboratories and models of epilepsy[12]. With this approach, we identified the histone methylase Enhancer of Zeste Homolog 2 (EZH2) as a potential driver of gene changes in dentate granule cells post-SE[17]. EZH2 was induced by an order of magnitude across epilepsy models. Transient pharmacological inhibition of EZH2 post-SE worsened epileptic phenotypes, suggesting that EZH2 induction plays a protective role in epileptogenesis. In addition to EZH2, our analysis predicted Signal Transducer and Activator of Transcription 3 (STAT3) to be a driver of gene activation across models of SE, hinting at an interplay between EZH2 and STAT3 signaling.

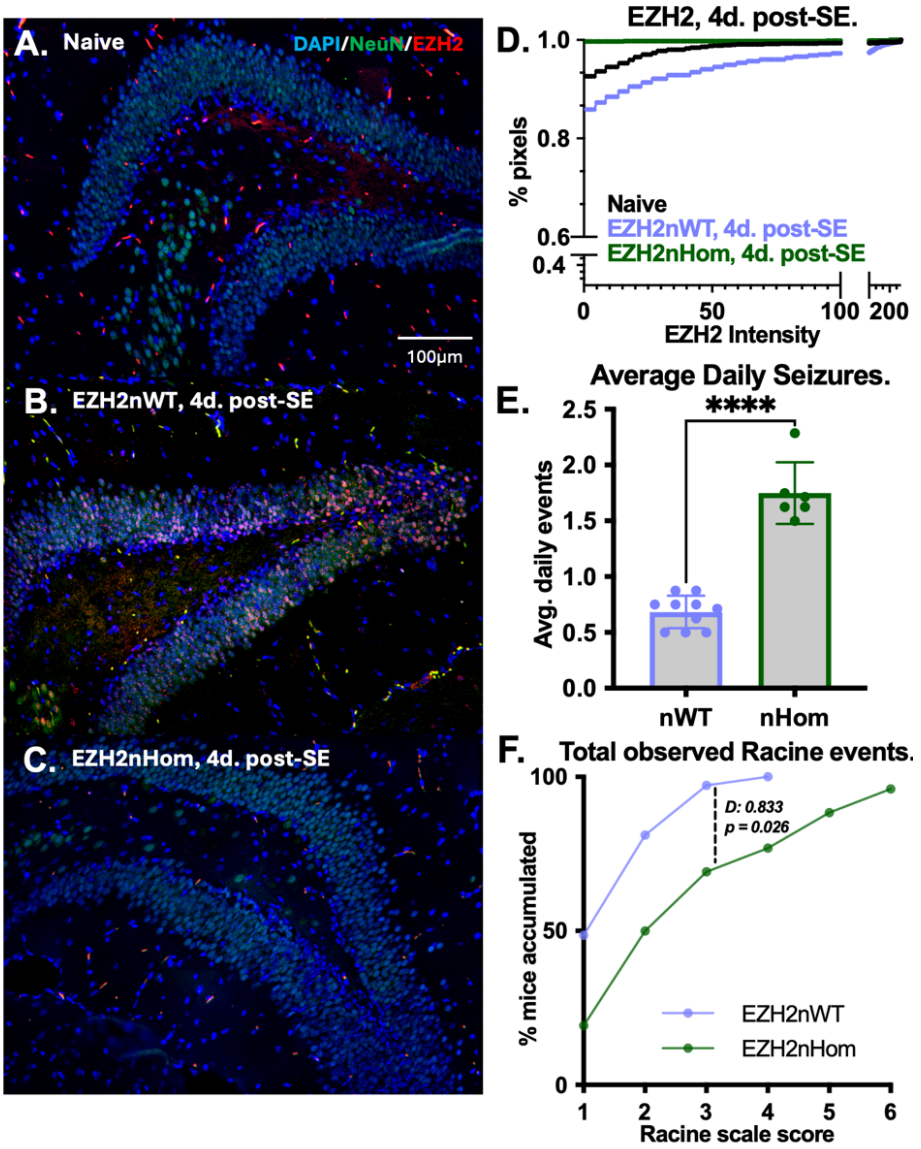

Fig. 1. Neuronal EZH2 induction after status epilepticus mitigates chronic disease progression. **(A-C)** Merged immunofluorescence images of the dentate gyrus labeling DAPI, NeuN, and EZH2 and **(D)** quantitation of EZH2 histograms from each panel. Statistical analysis was performed by Kruskal-Wallis test with Dunn's correction for multiple comparisons. Naïve mice showed low levels of EZH2 in neurons, while wildtype mice exhibited neuronal induction of EZH2 on day 4 post-SE ($p<10^{-4}$). EZH2nHom mice failed to show this induction, with EZH2 levels reduced compared to EZH2nWT mice 4d. post-SE ($p<10^{-4}$). **(E)** SRS activity was video recorded in epileptic EZH2nWT and nHom mice 5-7 weeks post-SE. EZH2nHom mice showed a 2.5-fold increase in seizure frequency (unpaired t-test; n=6-10). **(F)** Total observed Racine scale events for EZH2nHom and EZH2nWT mice were quantified as a frequency distribution. EZH2nHom mice had more severe seizures than WT mice. (Kolmogorov-Smirnov test; D:0.833; n=6-10).

Herein, we show that an inflammatory gene network centered around STAT3 appears acutely after SE and is negatively regulated by EZH2. STAT3 itself is activated robustly and quenched in an EZH2-dependent manner within days of SE. This is followed by an utterly unexpected resurgent activation with spontaneous seizures in the chronic period, accompanied by astrogliosis and microglial activation. Inhibiting the first wave of JAK/STAT signaling has no antiepileptogenic effect. However, briefly targeting the second wave of STAT3 activation in chronic epilepsy with the JAK inhibitor CP690550 results in an enduring, disease modifying suppression of spontaneous seizures, restoration of spatial memory, and rescue of neuropathological alterations.

RESULTS

Neuronal EZH2 induction protects against exacerbated epileptic phenotypes.

We previously identified the histone methyltransferase EZH2 as a potential driver of gene repression

post-SE, and EZH2 protein was robustly induced over a 10-day window post-SE in rats and mice across models of epilepsy. EZH2 induction was protective because pharmacological inhibition resulted in accelerated disease progression[17]. To determine the role of EZH2 in epilepsy, we crossed EZH2 floxed mice[30] with Syapsin1 Cre drivers[31] to delete EZH2 in mature neurons. Neuronal specificity of Cre expression was confirmed via crossing Syn1Cre with *flox*-STOP-*flox*-tdTomato mice and immunofluorescence. Staining for EZH2 confirmed reduced induction of neuronal EZH2 in EZH2nHom versus wildtype (EZH2nWT) mice post-SE (Fig. 1A-C) (see Fig. S1A-C for single-channel images).

To test the impact of neuronal EZH2 deletion on chronic disease, we monitored behavioral spontaneous seizures in FVB EZH2nWT and EZH2nHom mice by video from weeks 5-7 post-SE. EZH2nHom mice exhibited 2.5-fold greater seizure frequency compared to EZH2nWT mice (unpaired t-test; $p<10^{-4}$) (Fig. 1E). EZH2nHom mice also exhibited more severe Racine scale seizures than EZH2nWT mice (Kolmogorov-Smirnov test; D:0.833, $p<0.05$) (Fig. 1F). These data support the hypothesis that neuronal EZH2 induction post-SE is a protective response.

EZH2 tempers activation of the JAK/STAT pathway acutely post-SE.

To begin to understand the mechanism behind EZH2-mediated protection, we performed bulk RNAseq on whole hippocampal tissue from naïve and epileptic (4d. post-SE) EZH2nWT and EZH2nHom mice. Of the 10556 expressed genes, 6241 were found to be differentially expressed at an adjusted $p<10^{-2}$ (Likelihood Ratio Test) across the four conditions (saline, kainate, EZH2nWT, EZH2nHom). We used a community-based network approach to group genes into clusters. Leiden clustering generated 12 distinct groups (Fig. S2A). The grey, orange, gold, brown, skyblue, and purple clusters were generally repressed after SE, whereas the red, blue, indigo, yellow, and black clusters were generally increased. We focused on the Black cluster because these 439 genes were induced with SE in EZH2nWT mice but manifested an exaggerated induction with SE in EZH2nHom mice (Fig. 2A). We reasoned that these were genes whose expression is induced but tempered in the presence of EZH2 post-SE, and which undergo unfettered induction in the absence of EZH2.

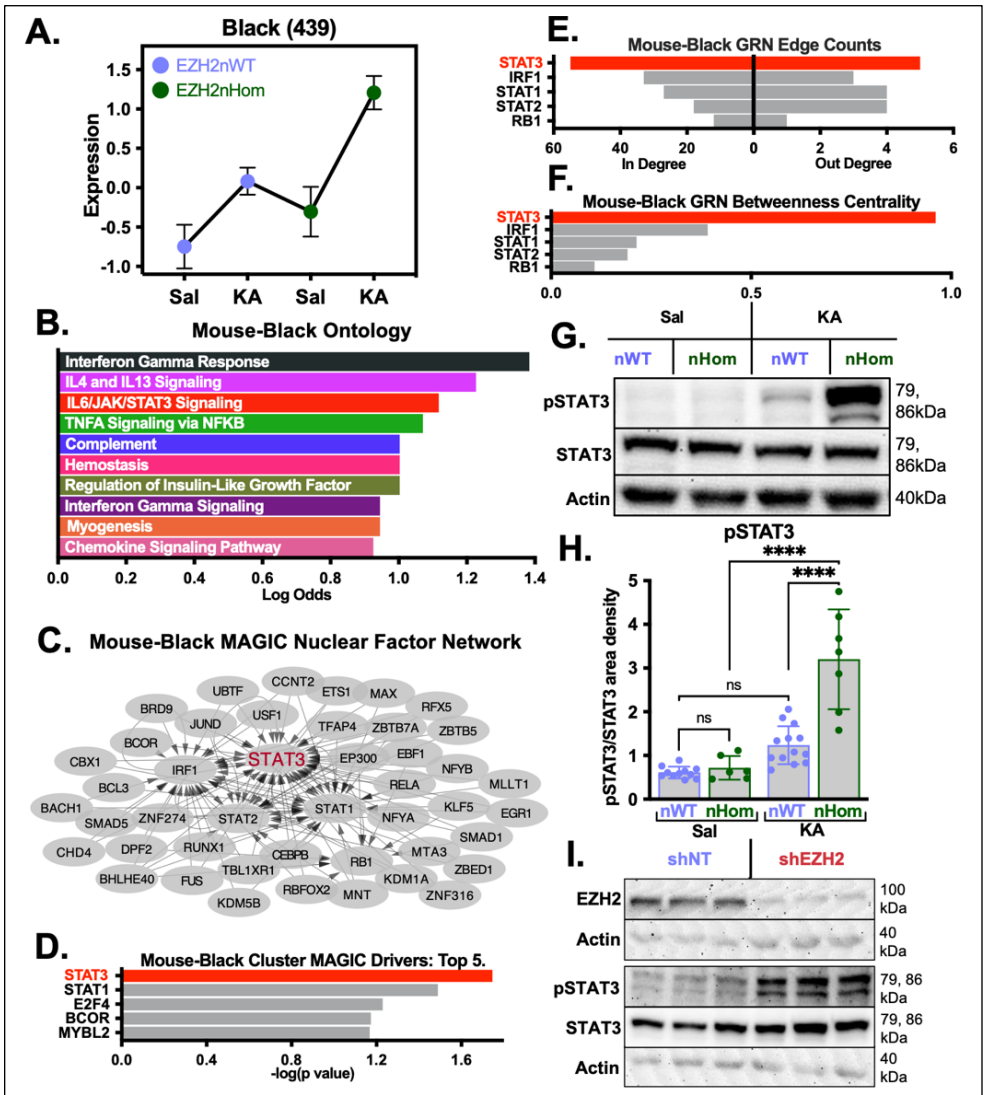

Fig. 2. STAT3 drives hyper-activation of pro-inflammatory gene networks in neurons acutely post-SE in EZH2 knockout mice. **(A)** Black Leiden cluster of 439 genes, one of twelve generated from 6241 differentially expressed genes (fold change >1.2x, adjusted $p<0.01$) across saline, kainate, EZH2nWT, and EZH2nHom conditions (see Fig. S3A). **(B)** Ontological analysis of genes in the Black cluster highlighted inflammatory processes. **(C)** MAGIC was used to determine which Factors control the expression of Black cluster genes, and positive hits were projected as a Gene Regulatory Network (GRN). **(D)** Top 5 Factors driving expression in the Black cluster sorted by –log(adjusted p value). **(E, F)** Factors were ranked by in degree and out degree counts, and betweenness centrality. **(G)** Hippocampi were harvested on day 4 post-SE from EZH2nWT and nHom mice for western blot analysis. **(H)** pSTAT3 was not altered by day 4 post-SE in EZH2nWT mice but was induced 4.5-fold in EZH2nHom mice (2-way ANOVA with Tukey's correction; n=7-12). **(I)** N2A cells were stably transfected with EZH2 shRNA (shEZH2) or non-targeting shRNA (shNT). Knockdown of EZH2 caused induction of pSTAT3 and total STAT3 protein (quantified in Fig. S5).

To understand the nature of genes comprising the Black cluster, we performed an ontological analysis (Fig. 2B). The 439 Black cluster genes were compared to gene lists associated with terms in the KEGG, Reactome, Biocarta and Hallmark databases. The resulting ontology network (see Fig. S2B) highlights the innate immune response (NFkB, Interferon Gamma, Complement) and inflammation (IL6 Jak Stat3) amongst others. The term 'IL6 Jak Stat3' was of particular interest because our previous work highlighted STAT3 as a driver of gene activation across models of epilepsy[17], and others have identified a pathological role for the JAK/STAT pathway in epileptogenesis[21,26,32-35].

To determine which transcription factors and cofactors (hereafter together referred to as 'Factors') control expression of Black cluster genes, we used MAGIC[36]. STAT3 was the highest scoring Factor predicted to drive gene expression in the Black cluster (Fig. 2D). When projected as a Gene Regulatory Network (GRN), such that an arrow projects from Factor X to Factor Y if the gene encoding Factor Y is a transcriptional target of Factor X, STAT3 stood out as a central node (Fig. 2C). Thus, STAT3 had the highest in-degree, out-degree, and total edge count (Fig. 2E) of any Factor in the network. Finally, we assessed the Betweenness Centrality[37] of the network to determine which Factors might be critical for information flow in the GRN. STAT3 had by far the largest Betweenness Centrality of any Factor (Fig. 2F).

Activation of the JAK/STAT pathway acutely post-SE in WT mice has been reported by others[17,33] (and Fig. 4A-C, S3A-F, S4A-B). To test for a neuronal EZH2-dependent change in JAK/STAT signaling, we performed western blot analysis on hippocampal lysates from 4d. post-SE EZH2nWT and EZH2nHom mice (Fig. 2G). Having undergone a burst of activation on day 1 post-SE, by day 4 post-SE phosphorylation of STAT3 at Tyr705 (pSTAT3) was almost back to baseline in EZH2nWT mice compared to naïve controls. In contrast, EZH2nHom mice exhibited sustained pSTAT3 induction (2-way ANOVA; 4.5-fold, $p<10^{-4}$) (Fig. 2H) in the absence of changes to total STAT3 (Fig. S3A). These results demonstrated an EZH2-dependent suppression of STAT3 activation in the days following SE.

To define the cell types in which STAT3 is activated after seizures, we performed immunofluorescence with DAPI, NeuN, and total STAT3 antibodies on day 1 post-SE hippocampi taken from mice injected with saline or kainic acid (Fig. S3F). We made use of the fact that total STAT3 protein is induced with STAT3 activation on day 1 post-SE (Fig. 4C), and so elevated total STAT3 protein was a proxy for activated STAT3. In both the dentate granule and CA1 pyramidal cell layer, we observed a robust induction of total STAT3 in NeuN-positive cells.

STAT3 was a central factor in the Black cluster GRN whereas, surprisingly, EZH2 was not. To understand how STAT3 hyperactivation occurred with EZH2 deletion, shRNA was used to knock down EZH2 in the Neuro2A (N2A) neuronal cell line. We observed robust diminution of EZH2 in knockdown cells (shEZH2) (unpaired t-test; 3.7-fold, $p<10^{-4}$) (Fig. 2I, quantified in S5A). This was associated with a marked increase in pSTAT3 levels (unpaired

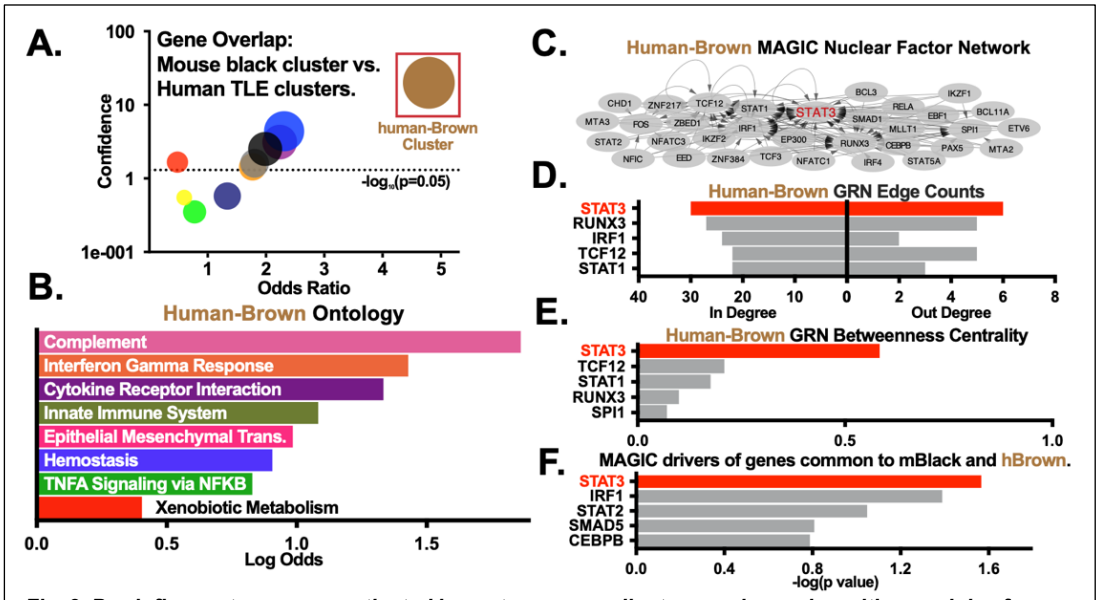

Fig. 3. Pro-inflammatory genes activated in acute mouse epileptogenesis overlap with a module of genes in chronic human temporal lobe epilepsy. **(A)** Comparison of 10 human TLE k-means gene clusters to the mouse Black cluster by Fisher Exact test. Plotting -log(adjusted p) versus odds ratio against the mouse Black cluster showed that the human Brown cluster is the most similar to the mouse Black cluster (Fisher exact; Odds:4.79, $p(adj)=1.2\times10^{-20}$). Dotted line shows p=0.05. **(B)** Ontological analysis of genes in the human Brown cluster highlighted inflammatory processes. **(C)** MAGIC GRN for Factors driving the human Brown cluster. **(D-E)** Factors were ranked by their in degree, out degree, and betweenness centrality. **(F)** STAT3 was the top driver predicted by MAGIC to drive expression of the 65 genes common to the mouse Black and human Brown clusters.

t-test; 2.4-fold $p<10^{-4}$) (quantified in S5B). This result suggested that EZH2 suppresses STAT3 activation in a cell-autonomous manner without circuit level alterations.

JAK/STAT signaling is reignited in chronic epilepsy.

To ascertain whether the mouse Black cluster has a counterpart in human epilepsy, we used whole transcriptome data from 129 ante-mortem human temporal lobectomy patients[17,38]. We used k-means clustering[39] to generate 10 gene clusters from the 7658 genes co-expressed across all samples (brown, blue, purple, skyblue, grey, orange, indigo, green, yellow, red). To test whether any of these human clusters corresponded to the mouse Black cluster, we performed Fisher exact tests to measure the degree of overlap between the 439 mouse Black cluster genes and the genes comprising each cluster of the human TLE dataset (Fig. 3A). The human Brown cluster showed the greatest overlap with the mouse Black cluster (Fisher exact; Odds: 4.79, $p=1.19\times10^{-20}$, 65 gene overlap). Ontological analysis highlighted terms broadly similar to the mouse Black cluster such as inflammation (Cytokine Receptor Interaction/Complement/Innate Immune System) and interferon signaling (Interferon Gamma Response) (Fig. 3B, S2C). Mirroring results of the mouse Black cluster, STAT3 had the highest in-degree, out-degree, and betweenness centrality of any Factor in the human Brown gene regulatory network (Fig. 3C-E). MAGIC called STAT3 as the highest scoring Factor driving expression of genes co-expressed between the mouse Black and human Brown clusters (Fig. 3F). Given that the mouse Black cluster is from samples harvested 4 days post-SE and the Brown cluster is from chronically epileptic humans, this data suggests that STAT3 influences disease both in acute epileptogenesis and chronic epilepsy.

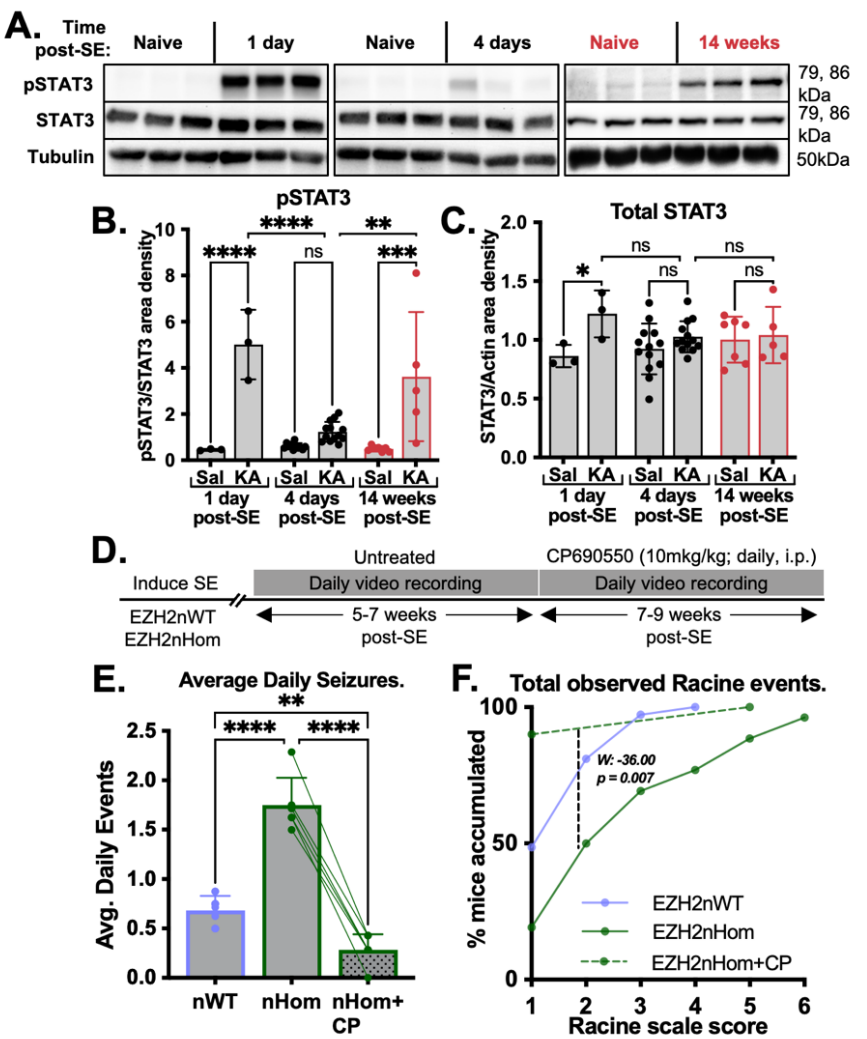

Fig. 4. JAK/STAT signaling is reactivated and targetable in chronic epilepsy. **(A)** Representative western blots for pSTAT3, total STAT3, and tubulin in naïve and epileptic mice at 1 day, 4 days, and 14 weeks post-SE. **(B-C)** pSTAT3 was induced 11-fold at 1 day and 7.3-fold at 14 weeks, but not induced 4 days post-SE. Total STAT3 was induced 1.4-fold on day 1 post-SE, but not 4 days and 14 weeks post-SE (2-way ANOVA with Tukey's correction; n=3-13). **(D)** SRS activity was monitored from 5-9 weeks post-SE, and nHom mice received daily CP690550 injections from 7-9 weeks post-SE. **(E)** CP690550 reduced seizure frequency by 80% in nHom mice, with nHom mice exhibiting seizure frequencies 58% below WT mice (1-way ANOVA with Tukey's correction; n=6-10). **(F)** Total observed Racine scale events represented as a frequency distribution. Daily CP690550 reduced seizure severity in nHom mice compared to pre-treatment (Wilcoxon matched pairs signed rank; W:-36.00, $p<0.01$, n=6) and WT mice (Mann Whitney test; U:119, $p<0.05$; n=6-10).

Following status epilepticus, robust activation of the JAK/STAT pathway diminishes within days[17,33] (Fig. 2G, 4A-B), yet MAGIC called STAT3 as a top factor driving gene expression in the chronically epileptic human Brown cluster. Therefore, we hypothesized that STAT3 activation reignites in chronic epilepsy. To test this, we collected hippocampi from mice 1 day, 4 days, and 14 weeks post-SE (Fig. 4A). On day 1 post-SE, pSTAT3 was induced 11-fold over naïve levels (2-way ANOVA; $p<10^{-4}$), but levels were diminished by day 4 post-SE (Fig. 4B). After the onset of spontaneous seizures at 14 weeks post-SE, we observed robust reactivation of STAT3 (7.3-fold, $p<10^{-3}$). Notably, EZH2 was not induced in chronically epileptic mice (Fig. S6A-B). This reactivation of JAK/STAT signaling corroborated the high degree of overlap between the acute mouse Black and chronic human Brown clusters. These results show that

JAK/STAT3 inflammatory signaling is transiently activated in neurons and glia after SE, abates over a period of days, but undergoes reignition with spontaneous seizures.

JAK/STAT signaling is a potent target in chronic epilepsy.

To screen for potential drugs that could suppress STAT3 activation and reignition, we took advantage of the constitutive STAT3 activation in shEZH2 cells (Fig. 2I). We incubated shNT and shEZH2 N2A cells with either WP1066 (an analogue of the JAK2 inhibitor AG490[40-42]) or CP690550 citrate (a small molecule inhibitor of JAK1/3 kinase activity[43-45]). WP1066 did not impact pSTAT3 in shEZH2 cells at any concentration tested (Fig. S7A-C). In contrast, 500nM CP690550 citrate reduced pSTAT3 levels in shEZH2 cells to that of vehicle-treated shNT cells (2-way ANOVA; 2.3-fold, $p<0.01$) (Fig. S7D-E). Importantly, total JAK1 was induced 1.6-fold in chronically epileptic hippocampi 14 weeks post-SE compared to naïve mice (2-way ANOVA; $p<10^{-3}$) (Fig. S6A,C).

To our knowledge, all attempts to pharmacologically modulate the JAK/STAT pathway in epilepsy have been conducted proximal to status epilepticus. Although mechanistically enlightening, this temporal window is largely irrelevant in clinical practice, and acute intervention has not been shown to prevent the onset of spontaneous seizures by others[26,32,35,46,47] (or Fig. S8A-C).

Instead, we asked whether CP690550 could rescue the increased seizure burden of EZH2nHom mice if administered during the chronic period. We recorded spontaneous seizures from weeks 5-7 post-SE in EZH2nWT and nHom mice, followed by two more weeks of recording during which the EZH2nHom mice received daily injections of CP690550 (Fig. 4D). Target engagement was confirmed by western blot (Fig. S9A-B).

Daily CP690550 treatment in the chronic period alleviated seizure severity in EZH2nHom mice (Wilcoxon paired; W:-36.0, $p<0.01$) and reduced seizure frequency by 80% (1-way ANOVA; $p<10^{-4}$) (Fig. 4E-F). Indeed, seizure frequency of drug-treated EZH2nHom mice was reduced to below EZH2nWT levels (1-way ANOVA; 1.9-fold, $p<0.01$). Given this robust seizure suppression when administered during the chronic period, we considered the possibility that CP690550 may simply be an anticonvulsant. To test this, we measured seizure threshold using both flurothyl and PTZ (pentylenetetrazole)[48,49] in mice pre-treated with vehicle or CP690550 (15mg/kg, i.p.) thirty minutes prior to testing. This time was chosen because peak plasma levels are observed 30 to 60 minutes after oral administration[50]. CP690550 pre-treatment had no effect on flurothyl or PTZ seizure threshold (Fig. S9C-D).

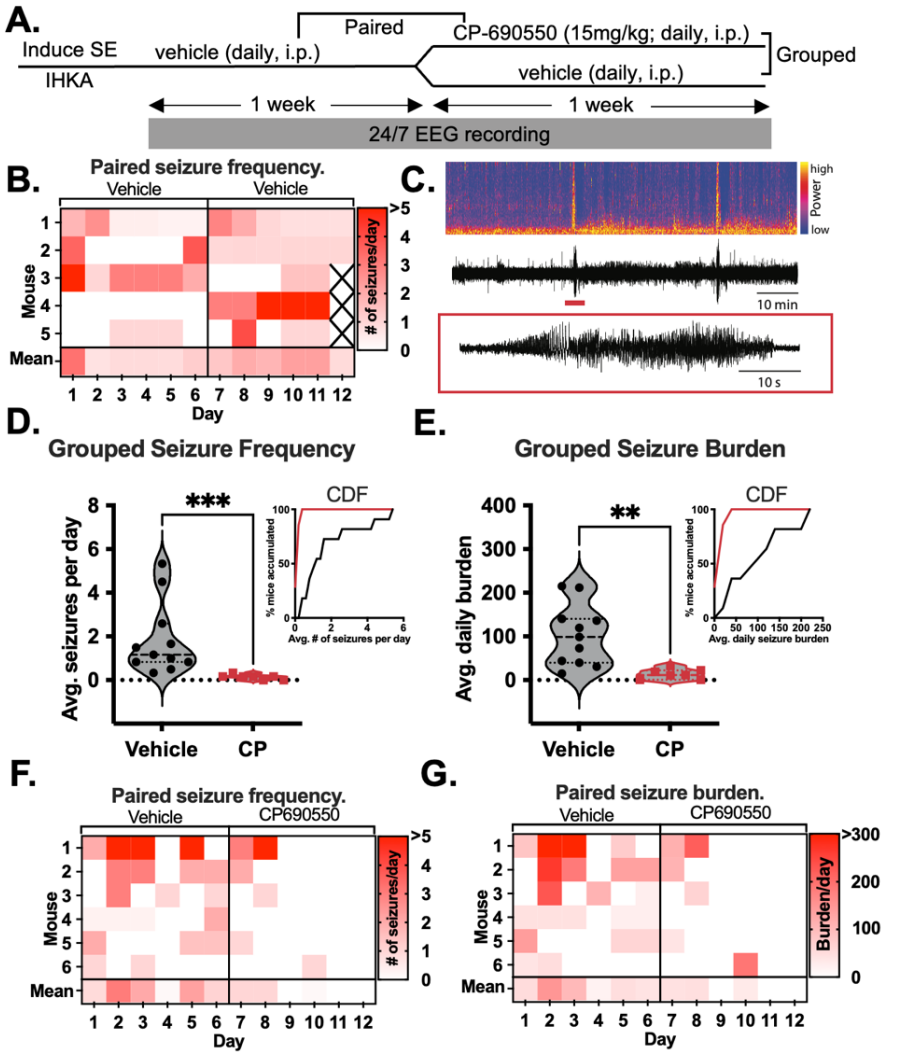

Fig. 5. CP690550 profoundly suppresses spontaneous seizures in epileptic wildtype mice. **(A)** SE was induced via IHKA. Under continuous EEG recording, vehicle was administered daily for one week followed by one week of daily vehicle or CP690550 treatment. **(B)** Vehicle-treated mice had seizures across both weeks of the experiment. **(C)** Example power spectrum, trace, and seizure. **(D-E)** Grouped comparisons for seizure frequency and burden were displayed as violin plots and cumulative frequency distributions (bin centers are marked). CP690550 treated mice showed a 13-fold reduction in seizure frequency and an 8-fold reduction in seizure burden (Kolmogorov-Smirnov test; D:0.91 (**Frequency**), D:0.71 (**Burden**); n=5-12). **(F-G)** Heat maps display paired data for seizure frequency and burden. Except for one seizure observed on day 10, CP690550 eliminated seizures after 2 days of treatment.

CP690550 enduringly suppresses electrographic and behavioral spontaneous seizures in chronically epileptic wildtype mice across models.

CP690550 treatment during the chronic period reduced seizure frequency in EZH2nHom mice to below wildtype levels, so we tested its effect on WT epileptic mice. Additionally, the finding that EZH2 is not induced in chronic epilepsy (see. Fig S6) led us to hypothesize that treatment during this window would be more effective than antiepileptogenic intervention. Wildtype mice were made epileptic via intrahippocampal kainate injections.

In a paradigm involving one week of daily vehicle (i.p.) administration initiated 10 days after SE induction, followed by an additional week of either vehicle or CP690550 injections (15mg/kg, i.p.) under continuous EEG recording (Fig. 5A), CP690550 treatment during the chronic period profoundly suppressed spontaneous seizures. CP690550-treated mice showed a 13-fold reduction in seizure frequency (Kolmogorov-Smirnov test; D:0.91, $p<10^{-3}$) and 8-fold reduction in burden (Kolmogorov-Smirnov test; D:0.71, $p<0.01$) over 1 week of recording (Fig. 5D-E). CP690550 treatment robustly reduced both spontaneous seizure frequency and burden in epileptic wildtype mice.

Additionally, while all animals experienced seizures during vehicle treatment, 80% of mice were seizure-free by the third day of CP690550 treatment (Fig. 5F-G). Animals treated with vehicle exhibited seizures throughout the experiment (Fig. 5B), contrasting with the profound reduction observed during CP690550 treatment.

Next, we tested the therapeutic effect of CP690550 in the systemic kainate model and adopted video-based behavioral seizure monitoring. These experimental modifications aimed to generalize the efficacy of CP690550 across epilepsy models and laboratories, minimize potential confounding effects introduced by headmount implantation and associated inflammation, and prioritize clinically relevant seizure endpoints. Seventeen mice were treated with 10 doses of CP690550 during weeks 11-12 post-SE, and were recorded daily for seizures. Fifteen mice (88%) responded to treatment (i.e., exhibited a seizure frequency and burden reduction of at least 50%). Two animals that did not exhibit a 50% reduction in seizure frequency and burden after two weeks of CP690550 treatment were classified as non-responders and omitted from the disease modification

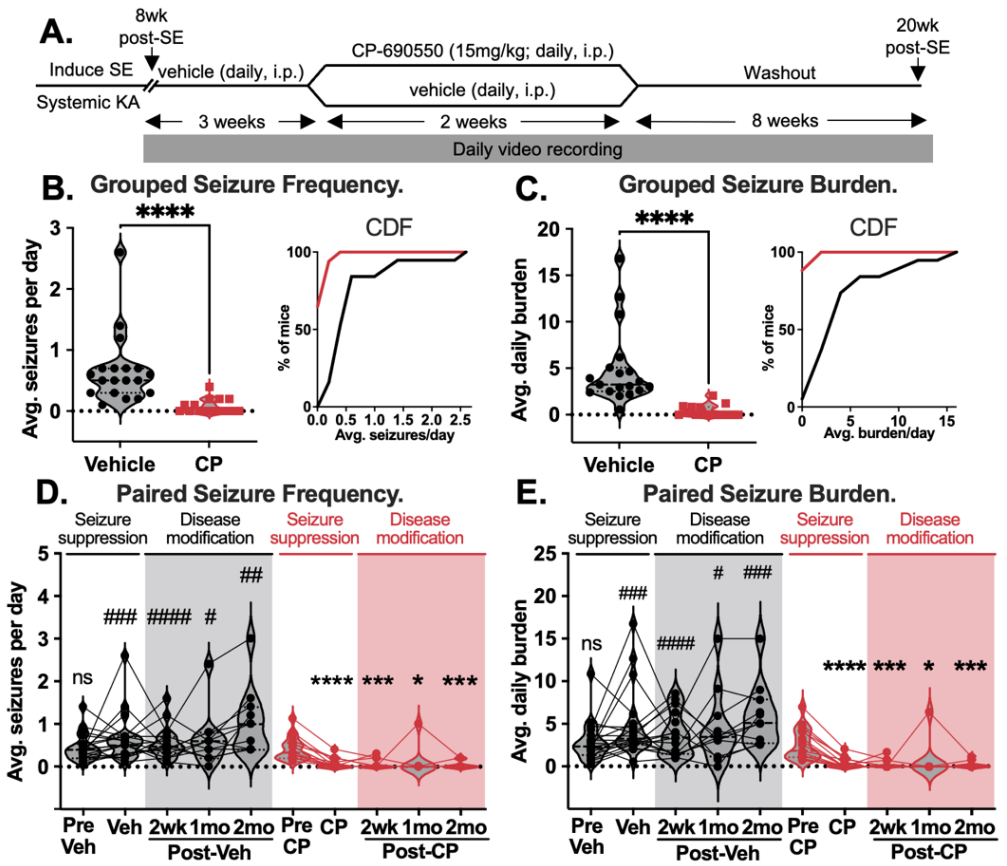

Fig. 6. CP690550 enduringly suppresses spontaneous seizures in epileptic wildtype mice at least 2 months post-washout. **(A)** SE was induced via systemic kainate, and behavioral seizures monitored by video from weeks 8-20 post-SE. Vehicle was administered from weeks 8-10 post-SE, followed by daily vehicle or CP690550 treatment weeks 11-12. After drug washout, video recording continued weeks 13-20 post-SE. **(B-C)** Grouped comparisons for seizure frequency and burden were displayed as violin plots and cumulative frequency distributions (bin centers are marked). Drug responders showed profound reductions in seizure frequency and burden (Kolmogorov-Smirnov test; **Frequency:** 9-fold, D:0.78, $p<10^{-4}$, **Burden:** 13.5-fold, D:0.89, $p<10^{-4}$; n=17-19). Paired seizure frequency **(D)** and burden **(E)** were displayed as violin plots with non-responders omitted (see Fig. S10, Table S1) (✱: CP-treated compared to pre-CP, #: vehicle compared to CP-treated) (2-way ANOVA with BKY correction; n=8-19). 2 weeks post-CP690550, mice showed a 10.5-fold reduction in frequency ($q<10^{-3}$) and a 15-fold reduction in burden ($q<10^{-3}$) compared to 2 weeks post-vehicle; 10 out of 13 mice (77%) were seizure-free during this time. At 2 months post-washout, drug-treated animals continued to exhibit a 21-fold reduction in seizure frequency ($q<10^{-3}$) and a 24-fold reduction in seizure burden ($q<10^{-3}$) compared to vehicle-treated mice (n=8-11).

phase of the experiment (see methods, and Fig. S10, Table S1 for analysis with all animals). Drug responders exhibited a 9-fold reduction in seizure frequency and a 12-fold reduction in seizure burden (Fig. 6B-C) (Kolmogorov-Smirnov test; **Frequency:** D:0.80, $p<10^{-3}$, **Burden:** D:0.86, $p<10^{-4}$).

We aimed to assess the durability of CP690550's profound effect on seizures. To do this, we withdrew drug and observed seizure frequency and burden from 13-20 weeks post-SE. CP690550 eliminated seizures completely in 58% of mice during treatment. Two weeks after drug withdrawal, 76% of drug responders were still seizure-free (2-way ANOVA; **Frequency:** 8-fold, $q<10^{-3}$, **Burden:** 10-fold, $q<0.01$) (Fig. 6D-E). Of the mice that were seizure free for the last 3 days of treatment, 10 out of 12 remained seizure free for 2 weeks after drug withdrawal. Some mice were harvested on the final day of treatment (12 weeks post-SE) and at two weeks post-washout (14 weeks post-SE) for experiments described in Figures 4 and 8 of this manuscript (see Methods).

Seizure suppression persisted to the end of recording. One month after drug withdrawal, one drug responder showed a relapse; the other seven mice were seizure free. Two months after the last dose of CP690550, we observed a 21-fold reduction in seizure frequency and a 25-fold reduction in seizure burden compared to vehicle-treated mice (2-way ANOVA; **Frequency:** $q<10^{-3}$; **Burden:** $q<0.01$). Together, these data suggest that CP690550 treatment may be a potent, novel therapeutic strategy for lasting seizure suppression.

CP690550 enduringly reverses cognitive comorbidities.

We asked whether chronically epileptic mice treated with CP690550 showed improvement of epilepsy-associated deficits in spatial memory. We tested working and short-term spatial memory at three time points: 1-2 weeks prior to SE, during CP690550 treatment at week 12 post-SE, and 2 weeks after drug washout at week 14 post-SE (Fig. 7A).

First, we asked whether CP690550 could rescue working spatial memory. To do this we measured spontaneous alternation (SA) in a previously described Y-maze testing paradigm[28,51,52]. Mice were placed in the starting arm of the maze facing the end of the arm and allowed to explore freely for 8 minutes. Sequential arm choices during exploration of a three-arm Y-maze are considered an indicator of spatial working memory because the innate curiosity of a healthy mouse promotes exploration of the most novel arm (i.e., the arm least recently visited)[51,52]. Distance traveled during each test was measured to ensure deficits in SA post-SE were not due to mobility impediments (Fig. S11A).

Chronically epileptic mice exhibited a 35% reduction in SA compared to naïve animals (1-way ANOVA; $q<10^{-3}$) (Fig. 7B). In contrast, daily CP690550 treatment rescued spatial memory by 31% ($q<0.01$), restoring performance to naïve levels (Fig. 7B).

Short-term memory requires that information collected during an experience be consolidated and accessible shortly thereafter[53]. Thus, we whether CP690550 treatment could rescue short-term consolidation. We measured short-term spatial memory with forced alternation (FA) tests in a Y-maze as previously described[3,51].

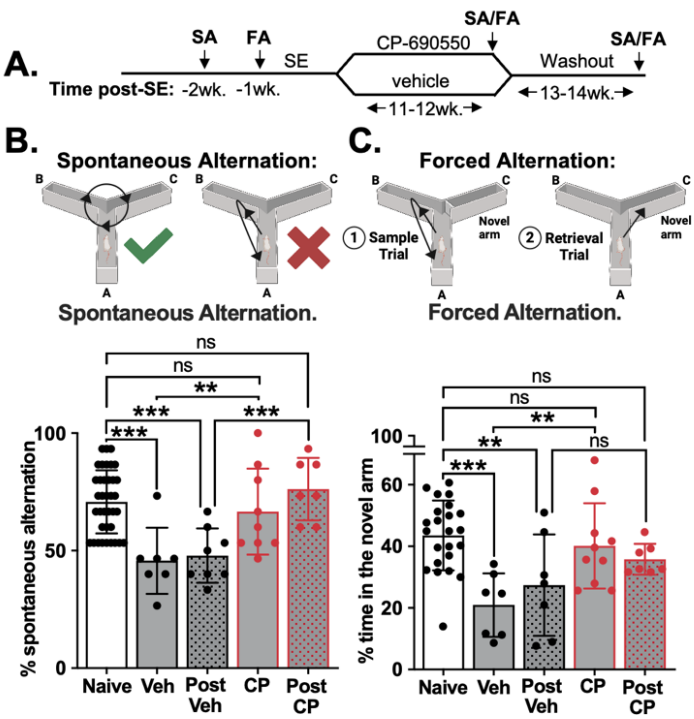

Fig. 7. CP690550 rescues working and short-term memory deficits in chronically epileptic mice. **(A)** Outline of experimental approaches for subsequent panels. **(B)** Spatial working memory was severely impaired in untreated chronically epileptic mice; SA was reduced 35% from baseline at week 12 post-SE and 32% at week 14 post-SE. Mice treated with CP690550 showed a 31% rescue in SA at week 12 post-SE and a 37% rescue at week 14, compared to vehicle-treated mice (1-way ANOVA with BKY correction; n=7-37). **(C)** Spatial short-term memory was likewise impaired in untreated mice; FA was reduced 52% from baseline at week 12 post-SE and 37% at week 14. In contrast, mice treated with CP690550 showed a 48% rescue in FA at week 12 post-SE compared to vehicle-treated mice (1-way ANOVA with BKY correction; n=7-23). Daily treatment with CP690550 rescued both SA and FA to levels indistinguishable from naïve mice both during treatment and after drug washout.

As with working memory, chronically epileptic mice showed profound deficits in short-term spatial memory, with time spent in the novel arm reduced by 52% at 12 weeks post-SE (1-way ANOVA; $q<10^{-3}$) compared to naïve mice (Fig. 7C). Mice treated daily with CP690550 exhibited a 48% increase ($q<0.01$) in time spent in the novel arm (Fig. 7C).

To assess the durability of CP690550's impact on cognition, we withdrew drug after week 12 post-SE. Two weeks after withdrawal, SA and FA tests were again performed. It should be noted that in naïve mice, repeated testing does not alter results for spontaneous or forced alternation, nor does CP690550 treatment in naïve mice (Fig. S11B-E). At 2 weeks post-washout, CP690550-mediated restorations in working memory persisted with a 37% increase in percent spontaneous alternations compared to vehicle-treated mice (1-way ANOVA; $q<10^{-3}$) (Fig. 7B). Short-term memory as measured by time spent in the novel arm remained indistinguishable from naïve animals two weeks after drug withdrawal, consistent with an ongoing protective effect of CP690550 (Fig. 7C). Together, these data show that targeting reignition of JAK/STAT signaling in chronic epilepsy enduringly suppresses both seizures and cognitive comorbidities.

CP690550 enduringly reverses epilepsy-related neuropathological alterations.

Profound seizure suppression observed with CP690550 treatment prompted us to assess the impact of this drug on histopathological markers of epilepsy. To address this question, we performed immunostaining for DAPI, GFAP, total STAT3, IBA1, and P2Y12 on hippocampi collected on the final day of treatment (Fig. 8A).

Chronically epileptic mice showed a profound induction of total STAT3 in neurons compared to naïve animals (Kruskal-Wallis test; $p<10^{-4}$), while CP690550 treatment reduced total STAT3 expression ($p<10^{-4}$) to levels indistinguishable from naïve mice (Fig. 8B). CP690550-mediated reductions in neuronal STAT3 expression were further accompanied by changes in astrogliosis and microglial activation. Both GFAP and IBA1 expression were reduced by CP treatment compared to vehicle (Fig. 8C-D). P2Y12 is a purinergic receptor selectively expressed on resident microglia[54] with reported roles in microglial homeostasis and neuroprotection[55-57], and its downregulation has been observed in association with both neurodegenerative disease[58] and seizures[59]. Herein, P2Y12 was downregulated in chronically epileptic vehicle-treated mice, with comparatively high levels observed in naïve and drug-treated mice (Fig. 8E).

At 2 months post-washout, histopathological differences between vehicle- and CP690550-treated mice persisted (Fig. 8F). Chronically epileptic mice showed induction of total STAT3 in neurons compared to naïve mice (Kruskal-Wallis test; $p<10^{-4}$), while mice 2 months post-CP690550 treatment continued to show reduced levels of neuronal STAT3 ($p<10^{-4}$) (Fig. 8G). Chronically epileptic mice showed profoundly increased GFAP and IBA1 expression compared to naïve mice (**GFAP:** $p<10^{-4}$; **IBA1:** $p<10^{-4}$). In contrast, 2 months post-CP690550 treatment, mice showed persistent reductions in both astrogliosis ($p<10^{-4}$) and microglial activation ($p<0.05$) compared to vehicle-treated mice (Fig. 8H-I). P2Y12 downregulation persisted in chronically epileptic mice, and high levels were observed in naïve and CP-treated mice 2 months post-washout (Fig. 8J). Concurrent with the profound seizure suppression effected by drug treatment, chronically epileptic mice treated with CP690550 exhibited enduring rescue of neuropathological changes associated with epilepsy and a lasting suppression of STAT3 expression long after drug withdrawal.

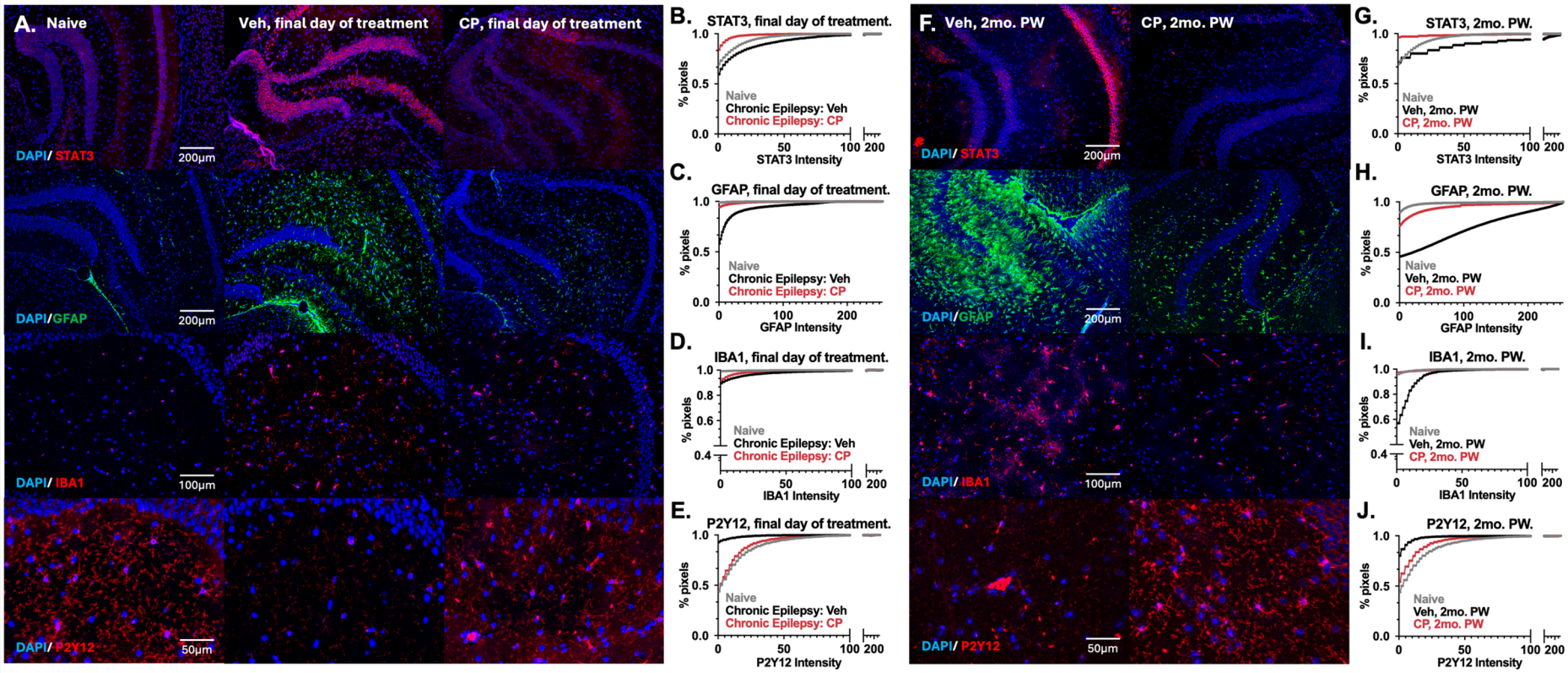

Fig. 8. CP690550 treatment enduringly suppresses astrogliosis and microglial activation at least 2 months post-washout. SE was induced via systemic kainate, and seizures monitored by video. Baseline seizure burden was established weeks 8-10 post-SE, followed by daily vehicle or CP690550 treatment weeks 11-12. Hippocampi were harvested 12 weeks post-SE (final day of drug or vehicle treatment). **(A)** Hippocampi were subjected to immunostaining for GFAP, IBA1, P2Y12, STAT3, and DAPI. Kruskal-Wallis tests with Dunn's correction for multiple comparisons were performed on quantitations in panels B-E, G-I. **(B)** At the end of drug treatment and at 2mo. post-washout, total STAT3 expression was reduced in CP-treated mice compared to chronically epileptic vehicle-treated mice ($p<0.01$). **(C)** Astrogliosis was reduced in CP-treated mice at the end of drug treatment compared to vehicle-treated mice ($p<10^{-4}$). **(D)** IBA1 expression was reduced in CP-treated mice at the end of drug treatment compared to vehicle-treated mice ($p<10^{-4}$). **(E)** P2Y12, a marker of microglial homeostasis, was downregulated in vehicle-treated chronically epileptic mice compared to naïve and CP-treated mice at the end of drug treatment ($p<10^{-4}$). **(F)** Hippocampi harvested 2 months post-vehicle and -CP were subjected to immunostaining for DAPI, GFAP, IBA1, and P2Y12. **(G-H)** GFAP ($p<10^{-4}$) and IBA1 ($p<0.05$) expression were both reduced in CP-treated mice compared to vehicle-treated mice. **(I)** P2Y12 was downregulated 2mo. post-vehicle compared to naïve and post-CP mice ($p<10^{-4}$).

501 502 503 504 505 506 507 508 509 510 511 512 513 514 515 516 517 518 519 520 521 522 523 524 525 526 527 528 529 530 531 532 533 534 535 536 537 538 539 540 541 542 543 544 545 546 547

DISCUSSION

We show that rapid induction of JAK/STAT3 signaling with SE is quenched by the chromatin modifier EZH2, but reignites in the chronic period. Targeting this resurgence with CP690550, an FDA-approved orally available drug, potently suppresses seizures, reverses cognitive comorbidities, and extinguishes astrocytic and microglial activation in an enduring manner. We provide evidence that the JAK inhibitor CP690550 is a novel, disease-modifying therapeutic agent for seizure suppression, cognitive restoration, and neuropathological rescue across epilepsy models.

EZH2 induction is protective after neurological insults.

After status epilepticus, EZH2 protein is induced in hippocampal pyramidal and dentate granule neurons across models of epilepsy[17]. Previously, we reported that treatment of mice with the SAM-competitive EZH2 inhibitor UNC-1999 exacerbated spontaneous seizures[17], and here we find that deletion of EZH2 in mature neurons has the same effect. Induction of Polycomb group (PcG) proteins has been studied in association with other brain insults. For example, sublethal ischemic insults lead to induction of Polycomb in mouse cortical neurons[60]. Further, sevoflurane (a volatile anesthetic that exerts positive allosteric modulation on $GABA_A$ receptors[61] and antagonizes NMDA receptors[62]) mediates protective induction of EZH2 and H3K27Me3 to attenuate hypoxic-ischemic brain injury and improve post-injury behavioral assessments in rats. These improvements are reversed when sevoflurane is given alongside the EZH2 inhibitor GSK126[63]. These studies, along with our findings, point to a potentially general protective role for EZH2 after CNS traumas.

EZH2 tempers activation of JAK/STAT signaling after status epilepticus.

EZH2 deletion in neurons results in large transcriptomic changes after SE (Fig. 2). The mouse Black gene cluster comprises genes induced after SE in EZH2nWT mice and hyper-induced in EZH2nHom mice after SE. This pattern suggests that EZH2 is responsible for tempering expression of genes in this cluster because its deletion results in their unfettered activation. The mouse Black cluster ontological analysis produces terms associated with innate immunity, neuroinflammation, and the JAK/STAT pathway. Network analysis places STAT3 in the center of the mouse Black GRN. Increased activation of STAT3 at Tyr705 as a result of EZH2 inactivation has also been observed in a transformed murine cell model of early T cell precursor acute lymphoblastic leukemia; EZH2 inactivation leads to enrichment of documented STAT3 target genes and exaggerated pSTAT3 induction with IL6 stimulation[64]. STAT-upstream receptors and kinases are also regulated by EZH2. In prostate cancer EZH2 represses IFNGR1 to dampen JAK2/STAT1 signaling, and its depletion restores expression of IFN target genes and pSTAT1[65]. The exact mechanism by which EZH2 tempers JAK/STAT signaling in the epileptic brain is a current focus of the lab.

Analysis of human TLE samples identifies a cluster of genes strikingly similar to the STAT3-driven mouse Black cluster; the human Brown cluster is a group of genes associated with innate immunity and neuroinflammation (Fig. 3). Like the mouse Black cluster, the most influential driver of gene expression is STAT3. The robust overlap between clusters of genes, one from frankly epileptic human samples and another from rodents in an early epileptogenic period, suggests a couple of insights. Firstly, STAT3-mediated epileptogenic mechanisms identified in mice are clinically relevant to the human population. Secondly, STAT3 drives gene changes both acutely after insult and in chronic epilepsy; this is supported by the identification of STAT3 as a driver of gene expression, its transient activation acutely post-SE, and its reactivation in chronic rodent epilepsy (Fig. 4). Furthermore, the failure to observe EZH2 induction in chronic epilepsy suggests its protection is limited to acute epileptogenesis (Fig. S6), as animals with intact neuronal EZH2 still go on to develop spontaneous seizures, and the same genes hyper-induced with EZH2 deletion after SE are widely co-expressed across drug refractory human TLE patients.

JAK/STAT signaling is reactivated in chronic epilepsy.

STAT3 phosphorylation is robustly induced on day 1 post-SE and diminished by day 4 post-SE (Fig. 4A-C). Its subsequent resurgence in chronic epilepsy occurs at least as early as 12 weeks post-SE and persists to at least 20 weeks post-SE (Fig. 4A-C, Fig. 8). It remains unclear whether reignition of JAK/STAT signaling precedes or follows the onset of spontaneous seizures. This would be difficult to assess because latency to spontaneous seizure onset after chemoconvulsant-induced SE varies widely by model, mouse strain, and delivery method[66,67]. In the kainate model of epilepsy[68,69], others have observed latencies to spontaneous seizures ranging from 5-30 days for the IHKA model and 10-30 days for the systemic kainate model[66]. Detection method also matters

because electrographic seizures typically arise earlier than "clinical" motor seizures. Mean latency to electrographic seizures ranges from 5-13 days post-SE[70-72], while mean latency to behavioral seizures is more variable, ranging from 10-77 days post-SE[66,70-73].

If STAT3 reactivation precedes the onset of spontaneous seizures, this suggests that inflammatory JAK/STAT signaling itself may drive the onset of seizure activity, and putative mechanisms by which this may occur have been explored by the Brooks-Kayal and Russek groups[21,74]. If STAT3 reactivation occurs after the onset of spontaneous seizures, then the profoundly enduring effect on seizures that we observe with CP690550 suggests that ongoing inflammation in chronic epilepsy is required for seizure propagation. In either case, STAT3 reactivation is targetable and potently disease modifying.

JAK/STAT signaling is a potent therapeutic target in chronic epilepsy.

Pharmacological inhibition of STAT3 prior to or during SE blunts, but does not prevent onset of spontaneous seizures[26]. Though mechanistically enlightening, this approach lacks clinical utility in the absence of reliable disease biomarkers. Attempts to genetically ablate the STAT3 SH2 domain[32] plateaued disease progression but did not reduce seizure burden, and the impact on comorbidities was unclear due to differences between naïve wildtypes and naïve STAT3-SH2 knockout mice[32]. Inhibiting the first wave of JAK/STAT signaling with CP690550 has no effect on spontaneous seizures and epilepsy-associated memory decline (Fig. S8D). Targeting the second wave of STAT3 activation in chronic epilepsy with the JAK inhibitor CP690550 results in an enduring suppression of spontaneous seizures, restoration of spatial memory, and reductions in multiple histopathological markers of inflammation (Fig. 5-8).

CP690550 profoundly suppresses seizures in chronically epileptic wildtype mice across models of epilepsy as measured by two different methods of seizure detection. In the systemic kainate model, CP690550 improved seizure frequency and burden in 15 out of 17 mice (88%); only two showed no response. Fig. S10 and Table S1 show that the potently disease modifying effect of CP690550 treatment persists even with non-responders included in the analysis. Following cessation of CP690550 treatment we observe robust disease modification for at least two months. The endurance of this protection will be the focus of future studies.

Our finding that CP690550 can be administered transiently in the chronic period to give lasting seizure protection would largely mitigate the risk of systemic immunological effects associated with long-term use of JAK inhibitors, as in rheumatoid arthritis (RA)[75]. RA patients may require 6 months to 2 years of CP690550 treatment before improvements begin to manifest[76,77]. In contrast, we observe profound disease modification after two weeks of daily CP690550 treatment. Deaths during or after vehicle or CP690550 treatment were noted and analyzed for any treatment effects. There was no significant difference in mortality between treatment groups (Log-rank Mantel-Cox test; Chi square:0.893, $p>0.05$) (Fig. S12). Given the rapid suppression of seizures, future studies will seek to shorten the course of treatment and address the impacts, if any, of the current treatment regimen on cardiac health[78] and immune function[79].

CP690550 restores working and short-term memory in chronically epileptic mice.

Herein, we show that in addition to profound seizure suppression, CP690550 treatment during the chronic period enduringly alleviates epilepsy-associated deficits in spatial memory. Notably, CP690550 administered acutely post-SE has no effect on short-term memory decline (Fig. S8D), highlighting the importance of this second, targetable window. Cognitive decline is not only a challenge with current epilepsy therapies, but also a leading comorbidity of epilepsy itself[80,81]. Despite recent advances, there is a continued, critical need for disease modifying agents that address comorbid behavioral and cognitive decline[7,82]. The mechanism(s) linking epilepsy to comorbidities is still unclear, but inflammation is a commonality across epilepsy and co-occurring conditions such as cognitive dysfunction[83,84], depression[85], anxiety[86], and schizophrenia[87]. Indeed, others have shown that suppression of key neuroinflammatory mediators such as COX2-associated pathways[28] and Complement 3-dependent synaptic remodeling[88] rescues aspects of cognitive function in preclinical rodent models of acquired epilepsy. To our knowledge, CP690550 is the first pharmacological agent that may be administered transiently several weeks after the onset of spontaneous seizures to rescue spatial memory for weeks after drug withdrawal.

CP690550 rescues neuropathological alterations in chronic epilepsy.

We assessed neuropathological alterations in chronic epilepsy by performing immunofluorescence on hippocampal tissue harvested from naive, vehicle-treated, and CP690550-treated chronically epileptic mice on

660 the final day of treatment. We observed a significant increase in the expression of STAT3, GFAP, and IBA1 in
661 vehicle-treated mice, indicating heightened inflammation and gliosis characteristic of chronic epilepsy[89-92].
662 Notably, STAT3 expression was primarily elevated in neurons. In contrast, CP690550-treated mice exhibited a
663 marked reduction in the levels of these markers, demonstrating the anti-inflammatory effects of CP690550.
664 Interestingly, P2Y12, which was downregulated in vehicle-treated mice, was upregulated in both naive and
665 CP690550-treated mice, suggesting a restoration of microglial homeostasis[55-57]. Two months after drug washout,
666 we repeated immunostaining for the same targets. Remarkably, expression patterns observed at the end of
667 treatment persisted, with CP690550-treated mice continuing to show reduced levels of STAT3, GFAP, and IBA1,
668 alongside sustained upregulation of P2Y12. These findings suggest an enduringly anti-inflammatory effect after
669 brief CP690550 treatment.
670
671 While activation of the JAK/STAT pathway in non-neuronal cells post-SE is well-characterized[20,34,93,94], the role
672 of STAT3 in neurogenic inflammation (Fig. 8, S3F) post-SE is not clear[32]. Cytokines released from glial cells
673 following seizures increase neuronal excitability[95], and type I IFNs increase excitability in neocortical pyramidal
674 neurons via PKC[96]. Others report that seizure-induced activation of the JAK/STAT pathway alongside
675 upregulation of BDNF reduces the number of gamma-aminobutyric acid (GABA) type A alpha1 receptors
676 expressed in neurons following seizures, influencing GABA(A)R-dependent inhibition[21]. This relationship is likely
677 reciprocal, with the reduction of neuronal STAT3 expression influencing inflammatory markers in non-neuronal
678 cells. For example, BDNF upregulated in neurons after seizures binds to TrkB receptors expressed by glial cells
679 to promote reactive phenotypes[97,98]. By dampening STAT3 activity in neurons, CP690550 may indirectly reduce
680 the reactivity of astrocytes and microglia, as indicated by the decreased levels of GFAP and IBA1 (Fig. 8).
681
682 **The advantage of CP690550 over other disease modifying agents.**
683 The persistence of CP690550's impact on seizures, cognition, and neuropathological alterations underscores its
684 potential as a disease-modifying agent. Existing anti-inflammatory drugs that have been used to suppress
685 seizures in human patients[22-25] or have shown antiepileptogenic potential[26-29] in rodents pose several drawbacks:
686 some or all are proposed only as supplemental therapies[22,23], risk worsened disease outcomes[23], show only
687 transient effects[24], or are effective in a small subset of epilepsy patients[23,25]. The disease modifying properties
688 of agents like dimethyl fumarate (DMF)[99] and sodium selenate[100] have also been reported. Like CP690550, DMF
689 is FDA-approved[101], and its administration in chronic epilepsy suppresses seizures during treatment and after
690 drug washout. Whereas DMF was able to enduringly suppress seizures when administered to chronically
691 epileptic rats, its impact on cognition with chronic administration was not tested, and administration at the time
692 of insult, as previously highlighted, has little clinical utility. CP690550 is distinguished compared to other drugs,
693 in that it appears to offer enduring benefits by mitigating inflammation long after drug discontinuation. This long-
694 term modulation of inflammatory markers is particularly notable, as it points to a profound and sustained impact
695 on the underlying neuropathological processes in epilepsy.
696
697 **Systemic inflammation in rheumatoid arthritis is associated with higher risk of epilepsy.**
698 CP690550 citrate is an FDA-approved drug for the treatment of rheumatoid arthritis and ulcerative colitis, and
699 evidence points to an association between peripheral inflammatory disease and risk for developing epilepsy.
700 Adjusted hazard ratios for developing epilepsy were compared between a cohort of 32,000 rheumatoid arthritis
701 (RA) patients and a cohort of sex- and age-matched controls; RA patients were at a significantly elevated risk[102].
702 Intriguingly, when RA patients were stratified by duration of nonsteroidal inflammatory drug (NSAID) use, those
703 who had used NSAIDs for less than 1.5 years were at the greatest risk, while those using NSAIDs for more than
704 5.8 years exhibited adjusted hazard ratios for epilepsy that were lower than the non-RA control cohort.
705
706 We have employed an open discovery, omics-based approach involving multiple animal models and laboratories
707 to identify drivers of disease, paired with a concerted effort to confirm relevance to human disease. With this
708 approach we identify EZH2 as a protective negative regulator of the JAK/STAT pathway in epileptogenesis. Our
709 current data is consistent with the hypothesis that CP690550 mitigates spontaneous seizures in chronic epilepsy
710 and is disease modifying. The cross-model, systems-based approach by which we identified JAK/STAT signaling
711 as a target of EZH2 and selected CP690550 suggests this drug may be useful across multiple human epilepsies
712 upon clinical translation. In sum, characterization of an endogenous, EZH2-mediated, protective response
713 across rodent models of epilepsy has highlighted a biphasic activation of JAK/STAT3 signaling: an early
714 induction and abatement after insult, followed by reactivation with chronic, spontaneous seizures. Transiently

targeting STAT3 reignition in chronic epilepsy with the FDA-approved drug CP690550 is potently seizure suppressing, memory restoring, and disease modifying.

METHODS

Bioinformatics

Reads were mapped to the mm39 build mouse genome and subjected to Likelihood Ratio Tests using Deseq2[103]. Transcripts per million were calculated and genes were classified as expressed if they had at least 3 TPM in all samples of any one of the 4 conditions (saline:WT, kainate:WT, saline:EZH2nHom, kainate:EZH2nHom). Deseq2 output was then filtered for only expressed genes and adjusted p-values were recalculated for the reduced number of genes. Genes with an adjusted p<.01 and 1.2-fold change were subjected to Leiden clustering with resolution=0.5 using the scanpy Leiden tool[104]. Ontology was performed on all clusters using Ontomancer (manuscript in preparation). Briefly, Biocarta, Hallmark, KEGG, and Reactome .gmt files were downloaded from https://www.gsea-msigdb.org/gsea/downloads.jsp. Gene sets associated with every term in the databases were collected. For each Leiden cluster, Scores (S_t) for each term, t, were calculated as:

$$S_t = \sqrt{(\log\ O_t)^2 + (-\log P_t)^2}$$

Where O_t and P_t, are the odds ratio and p values from Fisher exact tests for the overlap of Leiden cluster genes and genes for each term t. Only terms with odds ratios>1 and p values<0.05 were kept for further analysis. For each term, a gene list is generated containing the overlap of genes in the cluster and term, G_t. A term x term similarity matrix was generated where similarity between term i and j is the Fisher exact test log odds ratio $O_{i,j}$ for the intersection of genes in the terms G_i and G_j. This was converted to a network where nodes are terms. Edge weights were calculated as:

$$weight = (\log\,(O_{i.j})\,/\max\log O)^6$$

Where max log odds is the maximum log odds value across all comparisons. The 6 power was used to separate nodes for visualization. Networks were generated using the scanpy Leiden tool with resolution=2. Each community was named after the highest scoring term in that community. Networks were visualized via Python's networkx and Plotly tools.

MAGIC was performed on all clusters essentially as described[36] but with r=1, and GTFs were ignored. GTFs were defined as any ENCODE Factors containing the strings "TBP", "POL", "GTF", or "TAF".

Gene Regulatory Network was projected using Cytoscape[105] using MAGIC outputs. Factors were connected to their targets with edges defined as ChIP signal extracted from the Target Folder generated by MAGIC. Target genes of Factors that were not themselves Factors were removed to generate the GRN. Network statistics were calculated in Cytoscape[105]. ***Code for generation of Figures 2-3 will be made available on GitHub.***

Analysis of human TLE expression data.

GSE63808[38] from GEO contained 129 transcriptomes from resected hippocampal TLE tissue. Probes with an Illumina p-value<0.05 in at least 20% of samples were retained in the analysis; the probes were consolidated to gene symbols by taking the median probe expression value per symbol. These 9076 genes formed the background list for ontological and MAGIC analyses. Expression values were normalized by the median expression value in that sample. Genes kept for further analysis exhibited variance greater that the median coefficient of variance across all samples. The resulting 7658 unique genes were subjected to k-means clustering using the k-means tools from Sci-kit learn[106] to divide genes into 10 clusters (brown, blue, purple, skyblue, grey, orange, indigo, green, yellow, red).

Overlap between each of the 10 human TLE clusters with mouse Black cluster genes was measured by Fisher exact test with the Benjamini-Hochberg correction for multiple comparisons. Ontological and MAGIC analyses were performed on the highest-scoring human Brown cluster as described in the previous section.

Cell culture.

Growth conditions. Cells were grown in 5% CO_2 at 37°C. Neuro2a cells were grown in MEM (#10-009-CV Corning, Manassas, VA) with 1.0g/L glucose, 1.5g/L L-Glutamine, and 10% fetal bovine serum (#26140-079 Gibco, Grand Island, NY).

Lentiviral knockdown. Stable EZH2 knockdown in Neuro2a cells for western blot and RNA analysis was achieved using SMARTvector lentiviral delivery of shRNA per the manufacturer instructions. Puromycin selection began 48 hours after infection and maintained during cell expansion and experimentation. SMARTvector lentiviral mouse EZH2 mEF1a-TurboRFP shRNA (#V3SM7592-232015353, Dharmacon, Lafayette, CO) targeted the sequence *ATCGTAGTAAGTACCAATG*, and non-targeting mEF1a-TurboRFP control particles (#S10-005000-01) were used as an infection control.

Animal care

All animal procedures and experiments were performed with approval from the University of Wisconsin-Madison School of Medicine and Public Health Instructional Animal Care and Use Committee, or the Institutional Animal Care and Use Committee of Emory University, as appropriate, and according to NIH national guidelines and policies.

Transgenic mice. Cre-driver and EZH2 floxed mice were ordered from Jackson Laboratories (#003966, #022616, Bar Harbor, ME). Mice were bred on a C57BL6 background. Using the previously described Synapsin1-Cre system[31] *EZH2*$^{-/-}$; *Syn1Cre*$^{+/-}$ (EZH2nHom) mice were generated by mating *EZH2*$^{flox/flox}$*; Syn1Cre*$^{+/-}$ females with *EZH2*$^{flox/flox}$ males. *EZH2*$^{+/-}$*; Syn1Cre*$^{+/-}$ (EZH2nHet) mice were generated by mating *EZH2*$^{flox/+}$*; Syn1Cre*$^{+/-}$ females with *EZH2*$^{flox/flox}$ and *EZH2*$^{flox/+}$ males[107]. *EZH2*$^{+/+}$*; Syn1Cre*$^{+/-}$ (EZH2nWT) mice were generated from mating pairs containing an *EZH2*$^{flox/+}$ male. To assess Cre expression, we used a reporter mouse with a lox-P flanked STOP cassette preventing transcription of tdTomato (#007909 Jackson Laboratories) [108]. Reporter males were bred with *Syn1Cre*$^{+/-}$ females to generate Cre-positive animals and Cre-negative controls.

Repeated low-dose KA model. Male and female C57BL6 and FVB mice were bred and housed under a 12-hour light/dark cycle with access to food and water *ad libitum*. Mice were allowed to reach 4-6 weeks of age (C57BL6) 5-7 weeks of age (FVB) before undergoing experimentation. Kainate injections were performed at the same time of day (~10 A.M.), and mice were returned to home cages before the start of the dark cycle (~5 P.M.). Mice were housed with littermates for the duration of the experiment, with males and females separated at weaning.

We used a repeated low-dose kainate mouse model to induce SE. To begin, mice were weighed and singly housed in observation chambers for the duration of the injections. Mice were injected intraperitoneally (i.p.) with 5.0mg/kg synthetic kainic acid (KA) dissolved in 0.9% saline (#7065, Tocris Bioscience, Bristol, United Kingdom). At twenty-minute intervals, mice were given 5.0mg/kg injections of KA up to the third injection. The dosage was then reduced to 3.75mg/kg. Animals continued to receive 3.75mg/kg injections of KA every twenty minutes until each reached SE. The subsequent KA injection was skipped if an animal experienced two or more Class V seizures within a single twenty-minute interval. Injections resumed for the next round, unless the animal reached SE. During induction of SE, seizures were scored using a modified Racine Scale[109] where I = freezing, behavioral arrest, staring spells; II = head nodding and facial twitches; III = forelimb clonus, whole-body jerks or twitches; IV = rearing; V = rearing and falling; VI = violent running or jumping behavior. Animals were considered to have reached SE after experiencing at least five Class V or VI seizures within a 90-minute window. KA mice were observed for 1-2 hours after SE. Animals were injected with 0.9% saline (s.c.), and soft gel food was provided in home cages. In the days following injection, animals were weighed and injected with 0.9% saline (s.c.) if body weight decreased by more than 0.5g.

Pilocarpine model of status epilepticus. Adult C57BL6 mice (8-12 weeks old, Charles River) were injected with terbutaline (4 mg/kg ip, Sigma T2528) and methylscopolamine (4 mg/kg ip, Sigma S8502) to alleviate respiratory and cardiovascular effects of pilocarpine, then 30 min later received saline or pilocarpine (280 mg/kg i.p. as free base, Sigma P6503) as described[28]. After 1 hour of SE, seizures were interrupted by diazepam (10 mg/kg ip).

826
827 **IHKA model of status epilepticus.** The intrahippocampal kainic acid (IHKA) model was employed to
828 generate chronically epileptic mice as previously described[110]. Kainic acid (100 nL of 20 mM; vIHKA) or vehicle
829 (100 nL of sterile saline; vIHSA) was stereotaxically injected into the hippocampus using the following coordinate
830 (from Bregma): 3.6 mm posterior, -2.8 mm lateral, and 2.8 mm depth. Only mice which experienced status
831 epilepticus and went on to develop spontaneous recurrent seizures were used in the current study.
832
833 **Fluorothyl and PTZ seizure threshold testing.** Male and female C57BL6 mice were bred and housed
834 under a 12-hour light/dark cycle with access to food and water *ad libitum*. Animals were allowed to reach 4-6
835 weeks of age before undergoing experimentation. Fluorothyl seizure threshold tests were performed at the same
836 time of day (~10 A.M.), and mice were returned to home cages before 5 P.M. Mice were housed with littermates
837 for the duration of the experiment, with males and females separated at weaning. All seizure threshold tests
838 were video recorded, and seizure behavior was scored by a blinded observer. Two tests per mouse were
839 performed: the first at one week prior to kainate injections and the second at four days post-SE.
840 Seizure threshold tests were performed on male and female EZH2nWT, EZH2nHet, and EZH2nHom
841 mice using 100% bis(2,2,2-trifluoroethyl) ether (#287571, Sigma-Aldrich, St. Louis, MO). All tests were performed
842 in a fume hood. Mice were placed in an airtight 10L. Plexiglas chamber (8.5"X10.75"X6.75"). Fluorothyl was
843 infused into the chamber via a peristaltic pump at a rate of 40μL/minute onto a piece of Whatman filter paper
844 placed at the top of the chamber. The time to generalized tonic clonic seizure (GTCS) was recorded from the
845 start of fluorothyl infusion. Mice reached GTCS when they exhibited a complete loss of postural and motor
846 control. After experiencing a generalized tonic clonic seizure, mice were rapidly removed from the chamber, and
847 fluorothyl infusion was terminated. Mice were transferred to a recovery cage and kept isolated until motor control
848 and normal behavior returned (~10 minutes). Mice were returned to home cages after recovery. PTZ was
849 dissolved at 5mg/mL in 0.9% normal saline, and a single 45mg/kg dose was administered (i.p.). Time to
850 generalized tonic clonic seizure was recorded.
851
852 **Long-term video monitoring for spontaneous seizures.** Male and female FVB mice were bred and
853 housed under a 12-hour light/dark cycle with access to food and water *ad libitum*. Animals were allowed to reach
854 5-7 weeks of age before undergoing kainate injections. Starting at either week 5 or week 7 post-SE, video
855 recording for spontaneous seizures was performed at the same time of day (~10 A.M.), and mice were returned
856 to home cages before 5 P.M. Mice were singly housed in observation chambers for the duration of recording
857 with access to food and water. During daily CP690550 treatment, mice were weighed and injected daily before
858 recording began. Mice that did not exhibit at least 1 seizure per week (0.2/day) during the baseline recording
859 period or who died during recording were triaged from the analysis. Deaths during the chronic period after vehicle
860 or CP690550 treatment were noted and analyzed for any treatment effects (Fig. S12).
861 Videos were reviewed and scored by an experimenter blinded to treatment and genotype using the
862 modified Racine scale. In the experiments described by Figure 6, only Racine class IV-VI seizures were
863 recorded. For each mouse, daily seizure burden was calculated as: (Total # of seizures * Average seizure
864 duration (s))/(Total recording hours).
865
866 **CP690550 citrate treatment of KA mice.** Following kainate injections, an independent researcher (not
867 the experimenter) randomly assigned mice to drug and vehicle conditions, and prepared both solutions. Drug
868 and vehicle solutions were coded as "A" or "B." CP690550 citrate (tofacitinib citrate) (#4556, Tocris Bioscience,
869 Bristol, United Kingdom) was dissolved in a solution of 70% saline (0.9%)/15% ethanol/15% DMSO. The 70%
870 saline/15% ethanol/15% DMSO solution was administered as vehicle. The independent researcher provided the
871 blinded experimenter with the drug solutions and a list of all mice assigned to group A or B; this researcher did
872 not participate in any seizure threshold testing or spontaneous seizure video scoring. In acute experiments,
873 CP690550 or vehicle was delivered to mice intraperitoneally at 6, 18, 24, 48, and 72 hours post-SE. The first
874 dose of drug was given at 25mg/kg, and all others were 15mg/kg. In chronic experiments, CP690550 or vehicle
875 was delivered intraperitoneally daily for two weeks at 15mg/kg. Mice that did not respond to CP690550 treatment
876 with at least a 50% reduction in seizure frequency and burden were classified as non-responders and omitted
877 from the disease modification phase of the experiment. SRS analyses including non-responders can be found
878 in Fig. S10, and Table S1 includes mean seizure frequency, burden, and metadata for each animal. Of the 38
879 mice described in the seizure analysis, two CP690550-treated mice were non-responders and therefore omitted
880 from the disease modification arm of the experiment. Harvests on the final day of treatment decreased sample
881 sizes from n=19 to n=16 for vehicle-treated mice, and from n=17 to n=13 for CP690550-treated mice. Harvests

two weeks post-washout further decreased sample sizes from n=16 to n=11 for vehicle-treated mice, and from n=13 to n=8 for CP690550-treated mice.

Continuous EEG recording and seizure detection. At the time of stereotaxic IHKA or IHSA injections, mice were implanted with chronic EEG recording headmounts (Pinnacle Technology, cat. #8201) which were affixed to the skull with 4 screws: 2 screws serving as EEG leads placed in the anterior and posterior cortex, 1 as a reference ground, and 1 as the animal ground. The headmounts were secured with dental cement. 24/7 EEG recordings were collected at 4 KHz using a 100X gain preamplifier high pass filtered at 1KHz (Pinnacle Technology, cat. #8292-SE) and tethered turnkey system (Pinnacle Technology, cat. #8200).

Seizures were detected using a custom analysis pipeline developed in-house in python (seizy; https://github.com/neurosimata/seizy) as previously described[110]. Briefly, EEG traces were automatically detected using a thresholding method from traces that were downsampled (decimated) to 100 Hz and divided into 5 second segments. Power (2-40 Hz) and line length were used to identify seizures. Seizures were only included if two consecutive 5 second segments were classified as seizures (minimum 10 seconds length) and were manually verified by an experienced investigator with expertise in electrographic seizure detection. Seizure frequency was calculated as the # of seizures per day by measuring total number of seizures a mouse had over a 24-hour period. The average seizure duration was calculated by taking the mean seizure duration for each mouse in each recording period. For each mouse, seizure burden was calculated as: (Total # of seizures * Average seizure duration)/(Total EEG recording hours).

Y-maze cognitive testing. Working and short-term memory tests were performed at 3 time points: one (FA) or two (SA) weeks prior to induction of SE, post-CP690550 treatment (12 weeks post-SE), and post-washout (14 weeks post-SE). All tests were video recorded and analyzed by an experimenter blinded to treatment. Mice were habituated in the testing room for 30 minutes prior to all trials. We used spontaneous alternation to evaluate working memory and forced alternation to evaluate short-term memory; both tests occurred within a three-arm Y-maze. For spontaneous alternation, mice were placed in the starting arm of the maze and allowed to explore freely for 8 minutes. Sequential arm choices during exploration of a three-arm Y-maze are considered an indicator of spatial working memory because the innate curiosity of a healthy mouse promotes exploration of the arm least recently visited[28,51,52]. The number of choices resulting in a spontaneous alternation (e.g., an entry sequence of ABC but not ACA) was expressed as a percentage of the total number of choices.

After prolonged time in the Y-maze, habituation to novelty, and thus changes in motivation, can reduce the percentage of spontaneous alternations over time[28]. Testing naïve mice, we observed the transition from an exploratory phase to an escape phase, and the total number of alternations for each mouse ranged from 20-100. To mitigate the effects of habituation and the variance in total alternation, we analyzed only the first 15 alternations of each mouse. Mice that did not reach 15 alternations were removed from the dataset. Distance traveled during each 8-minute test was measured to ensure that deficits in SA post-SE were not due to mobility impediments.

Forced alternation (FA) tests depend on a mouse's ability to recall and apply spatial short-term memory, motivated by their innate curiosity. FA tests involved two 5-minute trials 30 minutes apart: a sample trial and a retrieval trial. In the sample trial, the mouse was placed in the starting arm and allowed to explore the maze with one arm blocked off. Between trials the maze was washed with 70% EtOH. In the retrieval trial, the previously blocked arm was opened, and the mouse was allowed to explore freely for 5 minutes. Mice that did not enter all three arms of the maze during the retrieval trial of FA tests were excluded from the dataset. FA tests were quantified as percentage of time spent in the novel arm.

Tissue isolation and homogenization

After KA seizure induction and/or treatment with CP690550 citrate, animals were sacrificed by rapid decapitation. Whole hippocampal hemispheres were harvested and flash-frozen in liquid nitrogen or on dry ice. Hippocampal tissue was lysed in Radioimmunoprecipitation Assay Buffer (RIPA: 50mM Tris, 150mM NaCl, 1% nonidet P-40, 0.5% sodium deoxycholate, 0.1% SDS) with mammalian protease inhibitor (1:1000, Sigma or 1860932 ThermoScientific) and phosphatase inhibitor (1:1000, Sigma or 78428 ThermoScientific). Protein from cell lines was harvested in Triton lysis buffer (3% 5M NaCl, 10% glycerol, 0.3% Triton X-100, 5% 1M Tris pH8.0) after PBS washes. Tissue was homogenized in lysis buffer by probe sonication (Fisher Scientific, Sonic Dismembrator, Model 100, Hampton, NH) on power 3 for two rounds, with 10 pulses per round. Supernatants were isolated by centrifugation and quantified using the DC Protein Assay (Bio-Rad, Hercules, CA) or BCA assay

(ThermoScientific 23227). Protein extracts were stored at -80˚C. 5x loading buffer (0.5mM Tris, 10% SDS, 50% glycerol, 10mM EDTA, and 1% beta-mercaptoethanol) was added to each sample to reach a 1x final concentration. Extracts in loading buffer were boiled at 95˚C for 5 minutes and stored for up to one month at -20˚C until run on an acrylamide gel.

Western blotting

Protein extracts in loading buffer were loaded at 20µg per lane and resolved by electrophoresis in hand-poured acrylamide gels with a 5% acrylamide stacking layer (125mM Tris pH6.8, 5% acrylamide, 0.01% ammonium persulfate, 0.01% SDS, 0.01% TEMED) and an 8% acrylamide separating layer (375mM Tris pH8.8, 8% acrylamide, 0.015% ammonium persulfate, 0.015% SDS, 0.08% TEMED). Gels were transferred to polyvinyl difluoride membranes (PVDF; Millipore, Bedford, MA) using Tris-glycine transfer buffer (20mM Tris, 1.5M glycine, 20% methanol). Membranes were blocked with 5% bovine serum albumin (Fisher Scientific, Fair Lawn, NJ) diluted in low-salt Tris-buffered saline (w/w TBST; 20mM Tris pH7.5, 150mM NaCl, 0.1% Tween 20) with mammalian protease inhibitor (1:2000) and phosphatase inhibitor (1:2000), or Odyssey blocking solution (LI-COR, 927-60001) for 1 hour at room temperature. Primary antibodies were diluted in the same blocking buffer and incubated with membranes overnight at 4˚C. Antibodies include: EZH2 (1:1000, #5426 Cell Signaling, Danvers, MA), phospho-STAT3 (Tyr705) (1:2000, #9145 Cell Signaling), total STAT3 (1:1000, #12640 Cell Signaling), JAK2 (1:1000, #3230 Cell Signaling), STAT1 (1:1000, #14994 Cell Signaling), pS727-STAT1 (1:1000, #8826 Cell Signaling), STAT2 (1:1000, #72604 Cell Signaling), pY1007/08-JAK2 (1:500, ab32101, Abcam, Cambridge, UK), Tubulin (1:1000, #T9026 Sigma-Aldrich), and Actin (1:10,000, #691001 MP Biomedicals). The next day, the membranes were washed three times in 1X TBST and incubated with horseradish peroxidase-conjugated goat-anti-mouse or -rabbit secondary antibodies for one hour at room temperature (1:10,000, Invitrogen #31430, #31460, Rockford, IL). Membranes were subsequently washed three times in TBST, and membranes were developed in SuperSignal West Femto ECL reagent (ThermoFisher, Waltham, MA). Bands were imaged using a ChemiDoc-It Imaging System (UVP Vision-Works, Upland, CA) and quantified using UVP Vision Works software or ImageJ. Band intensities were graphed and analyzed using Prism 9 software (GraphPad Software, La Jolla, CA).

RNA extraction and clean-up for whole hippocampal RNAseq

Hippocampi were harvested from saline- and kainate-treated EZH2nWT and EZH2nHom mice on day 4 post-SE (n=4-5 per treatment/genotype). RNA was extracted from hippocampal tissue with Trizol (#1559602, Life Technologies, Carlsbad, CA), and concentration was determined by spectrometry. This was followed by a treatment with DNase (#AM2238, Invitrogen). RNA clean-up was carried with the RNeasy Mini Kit (#74104, Qiagen, Hilden, Germany). Purified samples were submitted to the Gene Expression core at the University of Wisconsin-Madison Biotechnology Center for library preparation and sequencing (https://biotech.wisc.edu).

Immunofluorescence

Whole brains were harvested, bisected sagitally, fixed in 4% paraformaldehyde, dehydrated in a series of graded TBS-Tween/ethanol solutions, embedded in paraffin, sectioned at 5µm and subjected to immunofluorescence for NeuN, GFAP, total STAT3, and DAPI. Heat induced antigen retrieval was performed in a 10mM citric acid buffer (pH 6.0). After a blocking step, mouse anti-NeuN (1:200 ab104224 Abcam, or 1:500 MAB377 from Millipore), rabbit anti-STAT3 (1:500 #12640 Cell Signaling), rabbit anti-EZH2 (1:50 #5246 Cell Signaling), rabbit anti-IBA1 (1:600 #013-27691 Fujifilm), or rabbit anti-P2Y12 (1:200 #69766 Cell Signaling) primary antibodies were applied and incubated overnight at 4°C. Slides were washed with PBS then incubated with goat-anti-mouse Alexa Fluor 488 (ab150113 Abcam) and goat-anti-rabbit Alexa Fluor 594 (ab150080 Abcam) secondary antibodies at a concentration of 1:200 for one hour at room temperature, followed in some experiments by two-hour incubation at room temperature with Alexa Fluro 488-conjugated mouse anti-GFAP antibody (1:200 #53-9892-82 Invitrogen). Nuclear DNA was stained with DAPI (300 nM) or a DAPI-containing mounting media (#H-1200 Vector Laboratories, Burlingame, CA). Slides were imaged at 20-40x magnification using a fluorescent microscope (Nikon E600 microscope with fluorescence or Zeiss Axio Observer A1 epifluorescence microscope). Images were captured with Zeiss Axiovision or Cellsens software (Olympus Life Science Solutions, Center Valley, PA). Image analysis and processing were performed in ImageJ (NIH, https://imagej.nih.gov/ij/).

Statistical analysis

For all statistical analysis – with the exception of RNAseq data – $q<0.05$ or $p<0.05$ corrected for multiple comparisons was considered statistically significant (*p/q<0.05, **p/q<0.01, ***p/q<10^{-3}, ****p/q<10^{-4}). Data were graphed as mean ± standard deviation (SD) in Prism 9 software (Graphpad Software, La Jolla, CA). Statistical tests were also performed in Prism. Western blot, seizure threshold, and spontaneous seizure data was analyzed by t-test, 2-way ANOVA, or 1-way ANOVA, with Tukey's correction for multiple comparisons or the two-stage step-up method of Benjamini, Krieger, and Yekutieli. Cumulative frequency distributions were measured by Kolmogorov-Smirnov tests for unpaired data, and the Wilcoxon matched pairs signed rank test for paired data. All statistical tests were two-tailed.

Funding. Supported by CURE (AR), Lily's Fund (AR), NIH grant 1R01NS108756 (AR, RD) and R01NS105628, R01NS102937, and R21NS120868 (JM).

Conflict of Interest. JM serves on the Scientific Advisory Board and has a Sponsored Research Agreement with SAGE Therapeutics for work unrelated to this project. AR and RD have no conflicts of interest to declare.

References

1 Hirtz, D. *et al.* How common are the "common" neurologic disorders? *Neurology* **68**, 326 (2007). https://doi.org/10.1212/01.wnl.0000252807.38124.a3

2 Gavvala, J. R. & Schuele, S. U. New-Onset Seizure in Adults and Adolescents: A Review. *Jama* **316**, 2657 (2016). https://doi.org/10.1001/jama.2016.18625

3 French, J. A. *et al.* Antiepileptogenesis and disease modification: Clinical and regulatory issues. *Epilepsia Open* **6**, 483 (2021). https://doi.org/10.1002/epi4.12526

4 Beghi, E. & Giussani, G. Treatment of epilepsy in light of the most recent advances. *The Lancet. Neurology* **18**, 7 (2019). https://doi.org/10.1016/s1474-4422(18)30412-5

5 Chen, Z., Brodie, M. J., Liew, D. & Kwan, P. Treatment Outcomes in Patients With Newly Diagnosed Epilepsy Treated With Established and New Antiepileptic Drugs: A 30-Year Longitudinal Cohort Study. *JAMA neurology* **75**, 279 (2018). https://doi.org/10.1001/jamaneurol.2017.3949

6 Löscher, W. & Hönack, D. Profile of ucb L059, a novel anticonvulsant drug, in models of partial and generalized epilepsy in mice and rats. *European Journal of Pharmacology* **232**, 147 (1993). https://doi.org/10.1016/0014-2999(93)90768-d

7 Lamberty, Y., Margineanu, D. G. & Klitgaard, H. Absence of negative impact of levetiracetam on cognitive function and memory in normal and amygdala-kindled rats. *Epilepsy & Behavior: E&B* **1**, 333 (2000). https://doi.org/10.1006/ebeh.2000.0098

8 Park, S.-P. & Kwon, S.-H. Cognitive effects of antiepileptic drugs. *Journal of Clinical Neurology (Seoul, Korea)* **4**, 99 (2008). https://doi.org/10.3988/jcn.2008.4.3.99

9 French, J. A. *et al.* Characteristics of medial temporal lobe epilepsy: I. Results of history and physical examination. *Annals of Neurology* **34**, 774 (1993). https://doi.org/10.1002/ana.410340604

10 Trinka, E. *et al.* A definition and classification of status epilepticus--Report of the ILAE Task Force on Classification of Status Epilepticus. *Epilepsia* **56**, 1515 (2015). https://doi.org/10.1111/epi.13121

11 Hesdorffer, D. C., Logroscino, G., Cascino, G., Annegers, J. F. & Hauser, W. A. Risk of unprovoked seizure after acute symptomatic seizure: effect of status epilepticus. *Annals of Neurology* **44**, 908 (1998). https://doi.org/10.1002/ana.410440609

12 Dingledine, R. *et al.* Transcriptional profile of hippocampal dentate granule cells in four rat epilepsy models. *Scientific Data* **4** (2017). https://doi.org/10.1038/sdata.2017.61

13 Becker, A. J. *et al.* Correlated stage- and subfield-associated hippocampal gene expression patterns in experimental and human temporal lobe epilepsy. *The European Journal of Neuroscience* **18**, 2792 (2003). https://doi.org/10.1111/j.1460-9568.2003.02993.x

14 Borges, K., Shaw, R. & Dingledine, R. Gene expression changes after seizure preconditioning in the three major hippocampal cell layers. *Neurobiology of Disease* **26**, 66 (2007). https://doi.org/10.1016/j.nbd.2006.12.001

15 Hansen, K. F., Sakamoto, K., Pelz, C., Impey, S. & Obrietan, K. Profiling status epilepticus-induced changes in hippocampal RNA expression using high-throughput RNA sequencing. *Scientific Reports* **4** (2014). https://doi.org/10.1038/srep06930

16 McClelland, S. *et al.* The transcription factor NRSF contributes to epileptogenesis by selective repression of a subset of target genes. *eLife* **3** (2014). https://doi.org/10.7554/eLife.01267

17 Khan, N. *et al.* A systems approach identifies Enhancer of Zeste Homolog 2 (EZH2) as a protective factor in epilepsy. *PloS One* **14** (2019). https://doi.org/10.1371/journal.pone.0226733

18 Pfisterer, U. *et al.* Identification of epilepsy-associated neuronal subtypes and gene expression underlying epileptogenesis. *Nature Communications* **11** (2020). https://doi.org/10.1038/s41467-020-18752-7

19 Cid, E. *et al.* Sublayer- and cell-type-specific neurodegenerative transcriptional trajectories in hippocampal sclerosis. *Cell Reports* **35** (2021). https://doi.org/10.1016/j.celrep.2021.109229

20 Kumar, P. *et al.* Single-cell transcriptomics and surface epitope detection in human brain epileptic lesions identifies pro-inflammatory signaling. *Nature Neuroscience* **25**, 956 (2022). https://doi.org/10.1038/s41593-022-01095-5

21 Lund, I. V. *et al.* BDNF Selectively Regulates GABAA Receptor Transcription by Activation of the JAK/STAT Pathway. *Science Signaling* **1**, ra9 (2008). https://doi.org/10.1126/scisignal.1162396

22 You, S. J., Jung, D. E., Kim, H. D., Lee, H. S. & Kang, H. C. Efficacy and prognosis of a short course of prednisolone therapy for pediatric epilepsy. *European journal of paediatric neurology: EJPN: official journal of the European Paediatric Neurology Society* **12**, 314 (2008). https://doi.org/10.1016/j.ejpn.2007.09.003

23 Dubey, D. *et al.* Randomized Placebo-Controlled Trial of Intravenous Immunoglobulin in Autoimmune LGI1/CASPR2 Epilepsy. *Annals of Neurology* **87**, 313 (2020). https://doi.org/10.1002/ana.25655

24 Gayatri, N. A., Ferrie, C. D. & Cross, H. Corticosteroids including ACTH for childhood epilepsy other than epileptic spasms. *The Cochrane Database of Systematic Reviews* (2007). https://doi.org/10.1002/14651858.CD005222.pub2

25 Lai, Y.-C. *et al.* Anakinra usage in febrile infection related epilepsy syndrome: an international cohort. *Annals of Clinical and Translational Neurology* **7**, 2467 (2020). https://doi.org/10.1002/acn3.51229

26 Grabenstatter, H. L. *et al.* The effect of STAT3 inhibition on status epilepticus and subsequent spontaneous seizures in the pilocarpine model of acquired epilepsy. *Neurobiology of Disease* **62**, 73 (2014). https://doi.org/10.1016/j.nbd.2013.09.003

27 Jiang, J. *et al.* Suppressing pro-inflammatory prostaglandin signaling attenuates excitotoxicity-associated neuronal inflammation and injury. *Neuropharmacology* **149**, 149 (2019). https://doi.org/10.1016/j.neuropharm.2019.02.011

28 Varvel, N. H. *et al.* Preclinical development of an EP2 antagonist for post-seizure cognitive deficits. *Neuropharmacology* **224** (2023). https://doi.org/10.1016/j.neuropharm.2022.109356

29 Rojas, A., Ganesh, T., Lelutiu, N., Gueorguieva, P. & Dingledine, R. Inhibition of the prostaglandin EP2 receptor is neuroprotective and accelerates functional recovery in a rat model of organophosphorus induced status epilepticus. *Neuropharmacology* **93**, 15 (2015). https://doi.org/10.1016/j.neuropharm.2015.01.017

30 Shen, X. *et al.* EZH1 mediates methylation on histone H3 lysine 27 and complements EZH2 in maintaining stem cell identity and executing pluripotency. *Molecular Cell* **32**, 491 (2008). https://doi.org/10.1016/j.molcel.2008.10.016

31 Zhu, Y. *et al.* Ablation of NF1 function in neurons induces abnormal development of cerebral cortex and reactive gliosis in the brain. *Genes & Development* **15**, 859 (2001). https://doi.org/10.1101/gad.862101

32 Tipton, A. E. *et al.* Selective Neuronal Knockout of STAT3 Function Inhibits Epilepsy Progression, Improves Cognition, and Restores Dysregulated Gene Networks in a Temporal Lobe Epilepsy Model. *Annals of Neurology* (2023). https://doi.org/10.1002/ana.26644

33 Ahmed, M. M. *et al.* Altered Protein Profiles During Epileptogenesis in the Pilocarpine Mouse Model of Temporal Lobe Epilepsy. *Frontiers in Neurology* **12** (2021). https://doi.org/10.3389/fneur.2021.654606

34 Vishwakarma, S., Singh, S. & Singh, T. G. Pharmacological modulation of cytokines correlating neuroinflammatory cascades in epileptogenesis. *Molecular Biology Reports* **49**, 1437 (2022). https://doi.org/10.1007/s11033-021-06896-8

35 Martín-Suárez, S., Cortes, J. M. & Bonifazi, P. Blockage of STAT3 during epileptogenesis prevents GABAergic loss and imprinting of the epileptic state. *Brain: A Journal of Neurology* (2023). https://doi.org/10.1093/brain/awad055

36 Roopra, A. MAGIC: A tool for predicting transcription factors and cofactors driving gene sets using ENCODE data. *PLoS Comput Biol* **16** (2020). https://doi.org/10.1371/journal.pcbi.1007800

37 Freeman, L. C. Centrality in social networks conceptual clarification. *Social Networks* **1**, 215-239 (1978).

38 Johnson, M. R. *et al.* Systems genetics identifies Sestrin 3 as a regulator of a proconvulsant gene network in human epileptic hippocampus. *Nature Communications* **6** (2015). https://doi.org/10.1038/ncomms7031

39 Eisen, M. B., Spellman, P. T., Brown, P. O. & Botstein, D. Cluster analysis and display of genome-wide expression patterns. *Proceedings of the National Academy of Sciences of the United States of America* **95**, 14863 (1998). https://doi.org/10.1073/pnas.95.25.14863

40 Kupferman, M. E. *et al.* Therapeutic suppression of constitutive and inducible JAK\STAT activation in head and neck squamous cell carcinoma. *Journal of Experimental Therapeutics & Oncology* **8**, 117 (2009).

41 Hussain, S. F. *et al.* A Novel Small Molecule Inhibitor of Signal Transducers and Activators of Transcription 3 Reverses Immune Tolerance in Malignant Glioma Patients. *Cancer Research* **67**, 9630 (2007). https://doi.org/10.1158/0008-5472.can-07-1243

42 Iwamaru, A. *et al.* A novel inhibitor of the STAT3 pathway induces apoptosis in malignant glioma cells both in vitro and in vivo. *Oncogene* **26**, 2435 (2007). https://doi.org/10.1038/sj.onc.1210031

43 Dowty, M. E. *et al.* Preclinical to clinical translation of tofacitinib, a Janus kinase inhibitor, in rheumatoid arthritis. *The Journal of Pharmacology and Experimental Therapeutics* **348**, 165 (2014). https://doi.org/10.1124/jpet.113.209304

44 Meyer, D. M. *et al.* Anti-inflammatory activity and neutrophil reductions mediated by the JAK1/JAK3 inhibitor, CP-690,550, in rat adjuvant-induced arthritis. *Journal of Inflammation (London, England)* **7** (2010). https://doi.org/10.1186/1476-9255-7-41

45 Changelian, P. S. *et al.* Prevention of organ allograft rejection by a specific Janus kinase 3 inhibitor. *Science (New York, N.Y.)* **302**, 875 (2003). https://doi.org/10.1126/science.1087061

46 Tian, D.-S. *et al.* Chemokine CCL2-CCR2 Signaling Induces Neuronal Cell Death via STAT3 Activation and IL-1β Production after Status Epilepticus. *The Journal of Neuroscience: The Official Journal of the Society for Neuroscience* **37**, 7878 (2017). https://doi.org/10.1523/jneurosci.0315-17.2017

47 Raible, D. J. *et al.* JAK/STAT pathway regulation of GABAA receptor expression after differing severities of experimental TBI. *Experimental Neurology* **271**, 445 (2015). https://doi.org/10.1016/j.expneurol.2015.07.001

48 Rocha, L. Subchronic treatment with antiepileptic drugs modifies pentylenetetrazol-induced seizures in mice: Its correlation with benzodiazepine receptor binding. *Neuropsychiatric Disease and Treatment* **4**, 619 (2008). https://doi.org/10.2147/ndt.s2118

49 Baradaran Rahimi, V., Askari, V. R., Hosseini, M., Yousefsani, B. S. & Sadeghnia, H. R. Anticonvulsant Activity of Viola tricolor against Seizures Induced by Pentylenetetrazol and Maximal Electroshock in Mice. *Iranian Journal of Medical Sciences* **44**, 220 (2019).

50 Cohen, S., Zwillich, S. H., Chow, V., Labadie, R. R. & Wilkinson, B. Co-administration of the JAK inhibitor CP-690,550 and methotrexate is well tolerated in patients with rheumatoid arthritis without need for dose adjustment. *British Journal of Clinical Pharmacology* **69**, 143 (2010). https://doi.org/10.1111/j.1365-2125.2009.03570.x

51 Wolf, A., Bauer, B., Abner, E. L., Ashkenazy-Frolinger, T. & Hartz, A. M. S. A Comprehensive Behavioral Test Battery to Assess Learning and Memory in 129S6/Tg2576 Mice. *PloS One* **11** (2016). https://doi.org/10.1371/journal.pone.0147733

52 Hughes, R. N. The value of spontaneous alternation behavior (SAB) as a test of retention in pharmacological investigations of memory. *Neuroscience and Biobehavioral Reviews* **28**, 497 (2004). https://doi.org/10.1016/j.neubiorev.2004.06.006

53 Cowan, N. What are the differences between long-term, short-term, and working memory? *Progress in Brain Research* **169**, 323 (2008). https://doi.org/10.1016/s0079-6123(07)00020-9

54 Butovsky, O. *et al.* Identification of a unique TGF-β-dependent molecular and functional signature in microglia. *Nature Neuroscience* **17**, 131 (2014). https://doi.org/10.1038/nn.3599

55 Moore, C. S. *et al.* P2Y12 expression and function in alternatively activated human microglia. *Neurology(R) Neuroimmunology & Neuroinflammation* **2** (2015). https://doi.org/10.1212/nxi.0000000000000080

56 Cserép, C. *et al.* Microglia monitor and protect neuronal function through specialized somatic purinergic junctions. *Science (New York, N.Y.)* **367**, 528 (2020). https://doi.org/10.1126/science.aax6752

1151 57 Eyo, U. B. *et al.* Neuronal hyperactivity recruits microglial processes via neuronal NMDA receptors and microglial
1152 P2Y12 receptors after status epilepticus. *The Journal of Neuroscience: The Official Journal of the Society for*
1153 *Neuroscience* **34**, 10528 (2014). https://doi.org/10.1523/jneurosci.0416-14.2014
1154 58 Mildner, A., Huang, H., Radke, J., Stenzel, W. & Priller, J. P2Y12 receptor is expressed on human microglia under
1155 physiological conditions throughout development and is sensitive to neuroinflammatory diseases. *Glia* **65**, 375
1156 (2017). https://doi.org/10.1002/glia.23097
1157 59 Alves, M. *et al.* Expression and function of the metabotropic purinergic P2Y receptor family in experimental
1158 seizure models and patients with drug-refractory epilepsy. *Epilepsia* **58**, 1603 (2017).
1159 https://doi.org/10.1111/epi.13850
1160 60 Stapels, M. *et al.* Polycomb Group Proteins as Epigenetic Mediators of Neuroprotection in Ischemic Tolerance.
1161 *Science Signaling* **3**, ra15 (2010). https://doi.org/10.1126/scisignal.2000502
1162 61 Jenkins, A., Franks, N. P. & Lieb, W. R. Effects of temperature and volatile anesthetics on GABA(A) receptors.
1163 *Anesthesiology* **90**, 484 (1999). https://doi.org/10.1097/00000542-199902000-00024
1164 62 Brosnan, R. J. & Thiesen, R. Increased NMDA receptor inhibition at an increased Sevoflurane MAC. *BMC*
1165 *anesthesiology* **12** (2012). https://doi.org/10.1186/1471-2253-12-9
1166 63 Xue, H. *et al.* Sevoflurane post-conditioning alleviates neonatal rat hypoxic-ischemic cerebral injury via Ezh2-
1167 regulated autophagy. *Drug Design, Development and Therapy* **13**, 1691 (2019).
1168 https://doi.org/10.2147/dddt.s197325
1169 64 Danis, E. *et al.* Ezh2 Controls an Early Hematopoietic Program and Growth and Survival Signaling in Early T Cell
1170 Precursor Acute Lymphoblastic Leukemia. *Cell Reports* **14**, 1953 (2016).
1171 https://doi.org/10.1016/j.celrep.2016.01.064
1172 65 Wee, Z. N. *et al.* EZH2-mediated inactivation of IFN-γ-JAK-STAT1 signaling is an effective therapeutic target in
1173 MYC-driven prostate cancer. *Cell Reports* **8**, 204 (2014). https://doi.org/10.1016/j.celrep.2014.05.045
1174 66 Lévesque, M. & Avoli, M. The kainic acid model of temporal lobe epilepsy. *Neuroscience and Biobehavioral*
1175 *Reviews* **37**, 2887 (2013). https://doi.org/10.1016/j.neubiorev.2013.10.011
1176 67 Williams, P. A., Hellier, J. L., White, A. M., Staley, K. J. & Dudek, F. E. Development of spontaneous seizures after
1177 experimental status epilepticus: implications for understanding epileptogenesis. *Epilepsia* **48 Suppl 5**, 157
1178 (2007). https://doi.org/10.1111/j.1528-1167.2007.01304.x
1179 68 Ben-Ari, Y. & Lagowska, J. Epileptogenic action of intra-amygdaloid injection of kainic acid. *Comptes Rendus*
1180 *Hebdomadaires Des Seances De l'Academie Des Sciences. Serie D: Sciences Naturelles* **287**, 813 (1978).
1181 69 Ben-Ari, Y., Lagowska, J., Tremblay, E. & Le Gal La Salle, G. A new model of focal status epilepticus: intra-
1182 amygdaloid application of kainic acid elicits repetitive secondarily generalized convulsive seizures. *Brain*
1183 *Research* **163**, 176 (1979). https://doi.org/10.1016/0006-8993(79)90163-x
1184 70 Williams, P. A. *et al.* Development of spontaneous recurrent seizures after kainate-induced status epilepticus.
1185 *The Journal of Neuroscience: The Official Journal of the Society for Neuroscience* **29**, 2103 (2009).
1186 https://doi.org/10.1523/jneurosci.0980-08.2009
1187 71 Bertram, E. H. & Cornett, J. The ontogeny of seizures in a rat model of limbic epilepsy: evidence for a kindling
1188 process in the development of chronic spontaneous seizures. *Brain Research* **625**, 295 (1993).
1189 https://doi.org/10.1016/0006-8993(93)91071-y
1190 72 Smith, Z. Z., Benison, A. M., Bercum, F. M., Dudek, F. E. & Barth, D. S. Progression of convulsive and
1191 nonconvulsive seizures during epileptogenesis after pilocarpine-induced status epilepticus. *Journal of*
1192 *Neurophysiology* **119**, 1818 (2018). https://doi.org/10.1152/jn.00721.2017
1193 73 Hellier, J. L., Patrylo, P. R., Buckmaster, P. S. & Dudek, F. E. Recurrent spontaneous motor seizures after repeated
1194 low-dose systemic treatment with kainate: assessment of a rat model of temporal lobe epilepsy. *Epilepsy*
1195 *Research* **31**, 73 (1998). https://doi.org/10.1016/s0920-1211(98)00017-5
1196 74 Grabenstatter, H. L. *et al.* Effect of spontaneous seizures on GABAA receptor α4 subunit expression in an animal
1197 model of temporal lobe epilepsy. *Epilepsia* **55**, 1826 (2014). https://doi.org/10.1111/epi.12771
1198 75 Scott, B. L. & Becker, P. S. JAK/STAT Pathway Inhibitors and Neurologic Toxicity: Above All Else Do No Harm?
1199 *JAMA oncology* **1**, 651 (2015). https://doi.org/10.1001/jamaoncol.2015.1591
1200 76 van Vollenhoven, R. F. *et al.* Tofacitinib or adalimumab versus placebo in rheumatoid arthritis. *The New England*
1201 *Journal of Medicine* **367**, 508 (2012). https://doi.org/10.1056/NEJMoa1112072

1202 77 van Vollenhoven, R. *et al.* Evaluation of the Short-, Mid-, and Long-Term Effects of Tofacitinib on Lymphocytes in
1203 Patients With Rheumatoid Arthritis. *Arthritis & Rheumatology (Hoboken, N.J.)* **71**, 685 (2019).
1204 https://doi.org/10.1002/art.40780
1205 78 Ytterberg, S. R. *et al.* Cardiovascular and Cancer Risk with Tofacitinib in Rheumatoid Arthritis. *The New England*
1206 *Journal of Medicine* **386**, 316 (2022). https://doi.org/10.1056/NEJMoa2109927
1207 79 Kubo, S. *et al.* Janus Kinase Inhibitor Baricitinib Modulates Human Innate and Adaptive Immune System.
1208 *Frontiers in Immunology* **9** (2018). https://doi.org/10.3389/fimmu.2018.01510
1209 80 Murphy, G. G. Spatial Learning and Memory-What's TLE Got To Do With It? *Epilepsy Currents* **13**, 26 (2013).
1210 https://doi.org/10.5698/1535-7511-13.1.26
1211 81 Mula, M., Coleman, H. & Wilson, S. J. Neuropsychiatric and Cognitive Comorbidities in Epilepsy. *Continuum*
1212 *(Minneapolis, Minn.)* **28**, 457 (2022). https://doi.org/10.1212/con.0000000000001123
1213 82 Sanchez, P. E. *et al.* Levetiracetam suppresses neuronal network dysfunction and reverses synaptic and cognitive
1214 deficits in an Alzheimer's disease model. *Proceedings of the National Academy of Sciences of the United States of*
1215 *America* **109**, E2895 (2012). https://doi.org/10.1073/pnas.1121081109
1216 83 Marsland, A. L. *et al.* Brain morphology links systemic inflammation to cognitive function in midlife adults. *Brain,*
1217 *Behavior, and Immunity* **48**, 195 (2015). https://doi.org/10.1016/j.bbi.2015.03.015
1218 84 McAfoose, J. & Baune, B. T. Evidence for a cytokine model of cognitive function. *Neuroscience & Biobehavioral*
1219 *Reviews* **33**, 355 (2009). https://doi.org/10.1016/j.neubiorev.2008.10.005
1220 85 Slavich, G. M. & Irwin, M. R. From stress to inflammation and major depressive disorder: A social signal
1221 transduction theory of depression. *Psychological Bulletin* **140**, 774 (2014). https://doi.org/10.1037/a0035302
1222 86 Vogelzangs, N., Beekman, A. T. F., De Jonge, P. & Penninx, B. W. J. H. Anxiety disorders and inflammation in a
1223 large adult cohort. *Translational Psychiatry* **3**, e249 (2013). https://doi.org/10.1038/tp.2013.27
1224 87 Müller, N., Weidinger, E., Leitner, B. & Schwarz, M. J. The role of inflammation in schizophrenia. *Frontiers in*
1225 *Neuroscience* **9** (2015). https://doi.org/10.3389/fnins.2015.00372
1226 88 Dong, X. *et al.* Captopril alleviates epilepsy and cognitive impairment by attenuation of C3-mediated
1227 inflammation and synaptic phagocytosis. *Journal of Neuroinflammation* **19** (2022).
1228 https://doi.org/10.1186/s12974-022-02587-8
1229 89 Margerison, J. H. & Corsellis, J. A. Epilepsy and the temporal lobes. A clinical, electroencephalographic and
1230 neuropathological study of the brain in epilepsy, with particular reference to the temporal lobes. *Brain: A*
1231 *Journal of Neurology* **89**, 499 (1966). https://doi.org/10.1093/brain/89.3.499
1232 90 Blümcke, I., Beck, H., Lie, A. A. & Wiestler, O. D. Molecular neuropathology of human mesial temporal lobe
1233 epilepsy. *Epilepsy Research* **36**, 205 (1999). https://doi.org/10.1016/s0920-1211(99)00052-2
1234 91 Ravizza, T. *et al.* Innate and adaptive immunity during epileptogenesis and spontaneous seizures: evidence from
1235 experimental models and human temporal lobe epilepsy. *Neurobiology of Disease* **29**, 142 (2008).
1236 https://doi.org/10.1016/j.nbd.2007.08.012
1237 92 Altmann, A. *et al.* A systems-level analysis highlights microglial activation as a modifying factor in common
1238 epilepsies. *Neuropathology and Applied Neurobiology* **48** (2022). https://doi.org/10.1111/nan.12758
1239 93 Choi, J.-S. *et al.* Upregulation of gp130 and differential activation of STAT and p42/44 MAPK in the rat
1240 hippocampus following kainic acid-induced seizures. *Molecular Brain Research* **119**, 10 (2003).
1241 https://doi.org/10.1016/j.molbrainres.2003.08.010
1242 94 Wang, H. *et al.* LncRNA-UCA1 inhibits the astrocyte activation in the temporal lobe epilepsy via regulating the
1243 JAK/STAT signaling pathway. *Journal of Cellular Biochemistry* **121**, 4261 (2020).
1244 https://doi.org/10.1002/jcb.29634
1245 95 Iori, V., Frigerio, F. & Vezzani, A. Modulation of neuronal excitability by immune mediators in epilepsy. *Current*
1246 *Opinion in Pharmacology* **26**, 118 (2016). https://doi.org/10.1016/j.coph.2015.11.002
1247 96 Reetz, O., Stadler, K. & Strauss, U. Protein kinase C activation mediates interferon-β-induced neuronal
1248 excitability changes in neocortical pyramidal neurons. *Journal of Neuroinflammation* **11** (2014).
1249 https://doi.org/10.1186/s12974-014-0185-4
1250 97 Fernández-García, S. *et al.* Astrocytic BDNF and TrkB regulate severity and neuronal activity in mouse models of
1251 temporal lobe epilepsy. *Cell Death & Disease* **11** (2020). https://doi.org/10.1038/s41419-020-2615-9
1252 98 McNamara, J. O. & Scharfman, H. E. in *Jasper's Basic Mechanisms of the Epilepsies* (eds Jeffrey L. Noebels *et al.*)
1253 (National Center for Biotechnology Information (US), 2012).

99 Sandouka, S. *et al.* Repurposing dimethyl fumarate as an antiepileptogenic and disease-modifying treatment for drug-resistant epilepsy. *Journal of Translational Medicine* **21** (2023). https://doi.org/10.1186/s12967-023-04695-2

100 Casillas-Espinosa, P. M. *et al.* Disease-modifying effects of sodium selenate in a model of drug-resistant, temporal lobe epilepsy. *eLife* **12** (2023). https://doi.org/10.7554/eLife.78877

101 Fox, R. J. *et al.* Placebo-controlled phase 3 study of oral BG-12 or glatiramer in multiple sclerosis. *The New England Journal of Medicine* **367**, 1087 (2012). https://doi.org/10.1056/NEJMoa1206328

102 Chang, K.-H. *et al.* A Large-Scale Study Indicates Increase in the Risk of Epilepsy in Patients With Different Risk Factors, Including Rheumatoid Arthritis. *Medicine* **94** (2015). https://doi.org/10.1097/md.0000000000001485

103 Love, M. I., Huber, W. & Anders, S. Moderated estimation of fold change and dispersion for RNA-seq data with DESeq2. *Genome Biology* **15** (2014). https://doi.org/10.1186/s13059-014-0550-8

104 Wolf, F. A., Angerer, P. & Theis, F. J. SCANPY: large-scale single-cell gene expression data analysis. *Genome Biology* **19** (2018). https://doi.org/10.1186/s13059-017-1382-0

105 Assenov, Y., Ramírez, F., Schelhorn, S.-E., Lengauer, T. & Albrecht, M. Computing topological parameters of biological networks. *Bioinformatics (Oxford, England)* **24**, 282 (2008). https://doi.org/10.1093/bioinformatics/btm554

106 Pedregosa, F. *et al.* Scikit-learn: Machine Learning in Python. *Journal of Machine Learning Research* **12**, 2825 (2011).

107 Rempe, D. *et al.* Synapsin I Cre transgene expression in male mice produces germline recombination in progeny. *Genesis (New York, N.Y.: 2000)* **44**, 44 (2006). https://doi.org/10.1002/gene.20183

108 Madisen, L. *et al.* A robust and high-throughput Cre reporting and characterization system for the whole mouse brain. *Nature Neuroscience* **13**, 133 (2010). https://doi.org/10.1038/nn.2467

109 Racine, R. J. Modification of seizure activity by electrical stimulation. II. Motor seizure. *Electroencephalography and Clinical Neurophysiology* **32**, 281 (1972). https://doi.org/10.1016/0013-4694(72)90177-0

110 Basu, T. *et al.* Hypothalamic-pituitary-adrenal axis dysfunction worsens epilepsy outcomes and increases SUDEP risk. (Neuroscience, 2022).

SUPPLEMENTAL FIGURES

S1. Conditional knockout diminishes EZH2 induction post-SE.

S2. Leiden clusters and ontology networks for the mouse-Black and human-Brown clusters.

S3. STAT3 is induced in neurons, and other STAT family proteins are hyper-induced in EZH2nKO mice.

S4. Transient induction of STAT3 in wildtype animals is observed across models of SE.

S5. Western blot quantifications in shNT and shEZH2 N2A cells.

S6. JAK1 but not EZH2 is induced in chronic epilepsy.

S7. JAK1/3 but not JAK2 activity is required for hyper-activation of STAT3 in the absence of EZH2.

S8. Transient CP690550 treatment acutely post-SE does not alter epileptogenesis in wildtype mice.

S9. CP690550 target engagement and threshold testing with pre-treatment.

S10. Long-term SRS data for both responders and non-responders to CP690550 in the systemic kainate model.

S11. Distance traveled is not correlated with deficits in spontaneous alternation post-SE, and SA and FA results are not altered with repeated testing or CP690550 treatment in naïve mice.

S12. CP690550 treatment does not increase mortality in chronically epileptic mice.

SUPPLEMENTAL INFORMATION

Table S1. Tabulated daily seizure frequency, burden, and metadata for responders and non-responders to CP690550 in the systemic kainate model.

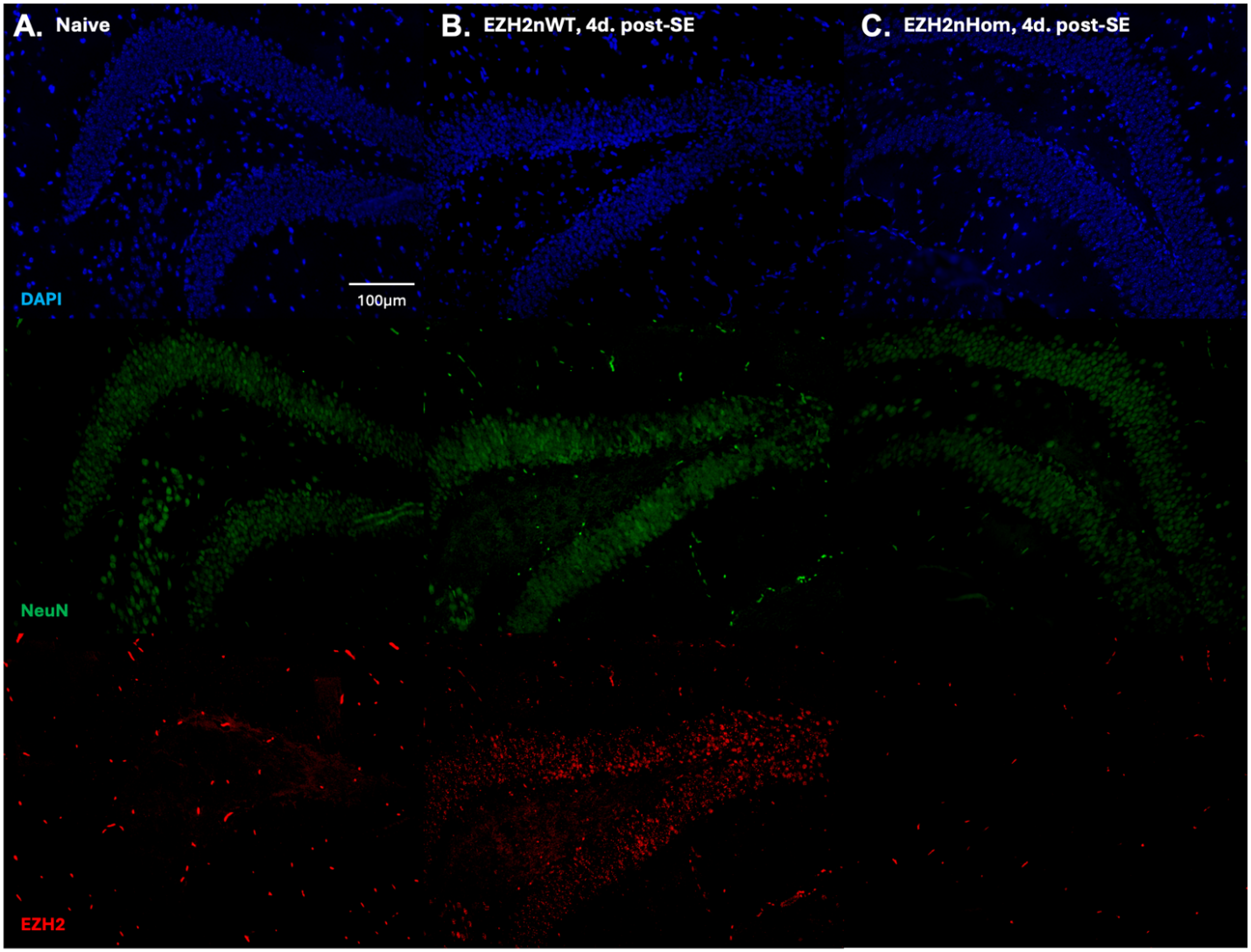

Fig. S1. Conditional knockout diminishes EZH2 induction post-SE. **(A-C)** Single-channel images of the dentate gyrus labeling DAPI, NeuN, and EZH2 in **(A)** naïve mice, **(B)** EZH2nWT mice 4 days post-SE, and **(C)** EZH2nHom mice 4 days post-SE.

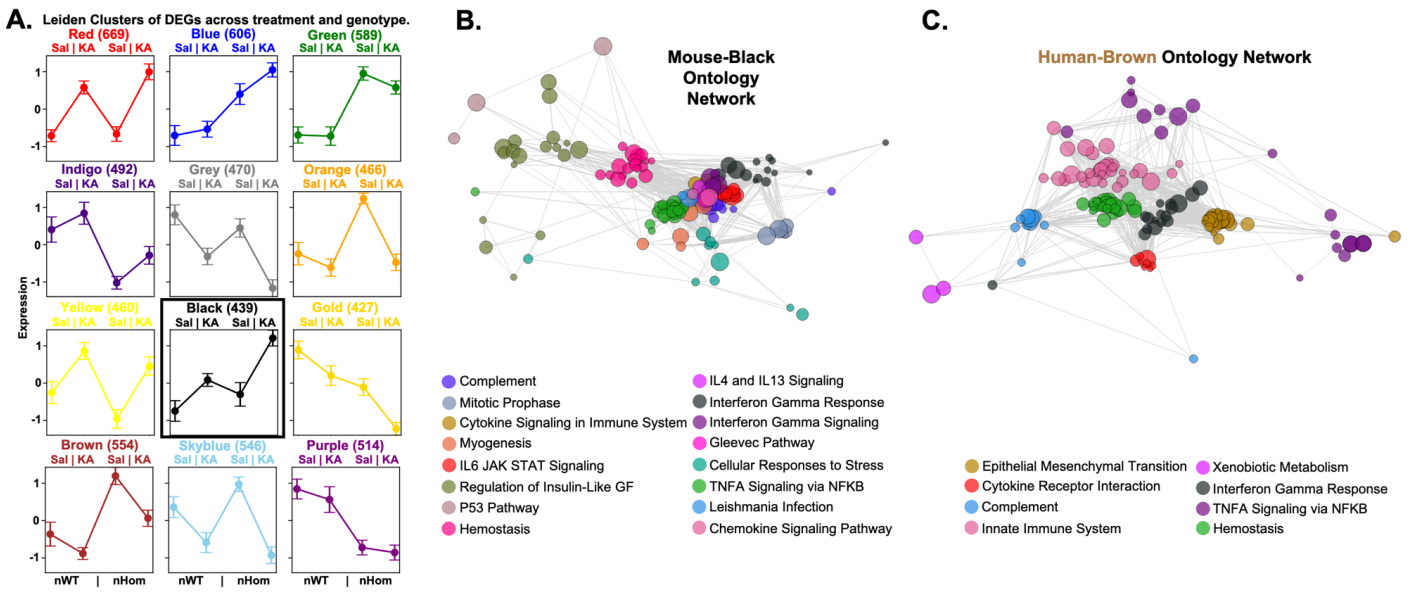

Fig. S2. Leiden clusters and ontology networks for the mouse-Black and human-Brown clusters. **(A)** Leiden clusters from 6241 differentially expressed genes (fold change >1.2x, adjusted p<0.01) across saline, kainate, EZH2nWT, and EZH2nHom conditions. **(B)** The 439 mouse-Black cluster genes and **(C)** 850 human-Brown cluster genes were compared to gene lists associated with terms in KEGG, Reactome, Biocarta, and Hallmark databases; terms with an odds ratio>1 and p<0.05 across all databases were sorted into ten communities via a network approach. Community names are the ontological term with the highest odds ratio in the community.

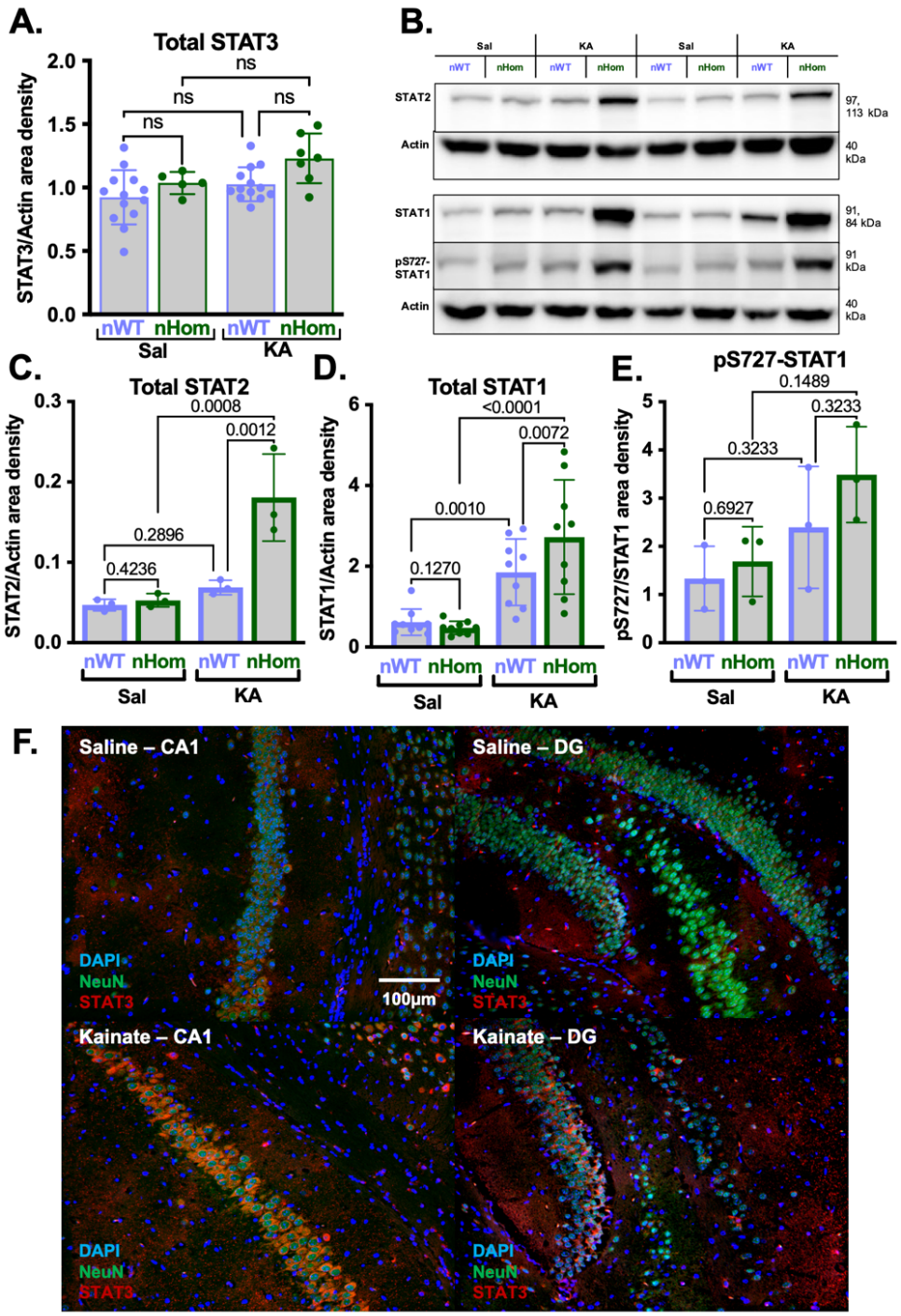

Fig S3. STAT3 is induced in neurons, and other STAT family proteins are hyper-induced in EZH2nKO mice. **(A)** Total STAT3 levels were not altered by treatment or genotype on day 4 post-SE (2-way ANOVA with Tukey's correction; n=5-13). **(B)** Representative western blots for total STAT2, total STAT1, phospho-STAT1 (S727) and beta-actin on day 4 post-SE. For all proteins quantified in panels C-E, deletion of an EZH2 allele did not alter protein levels in naïve animals. **(C)** Total STAT2 was induced after SE in EZH2nHom mice by 3.4-fold, or 2.6-fold greater than WTs post-SE (2-way ANOVA with Tukey's correction; n=3). **(D)** Total STAT1 protein was induced by 5.7-fold in EZH2nHom mice post-SE, or 1.5-fold greater than WTs post-SE (2-way ANOVA with Tukey's correction; n=9). **(E)** pS727-STAT1 was not robustly altered across the four conditions (2-way ANOVA; n=3). **(F)** 20x images of the CA1 pyramidal cell layer (CA1) and dentate gyrus (DG). Hippocampal slices were collected on day 1 post-SE from saline- and KA-injected mice; immunofluorescence was performed to detect nuclear DNA, NeuN, and total STAT3.

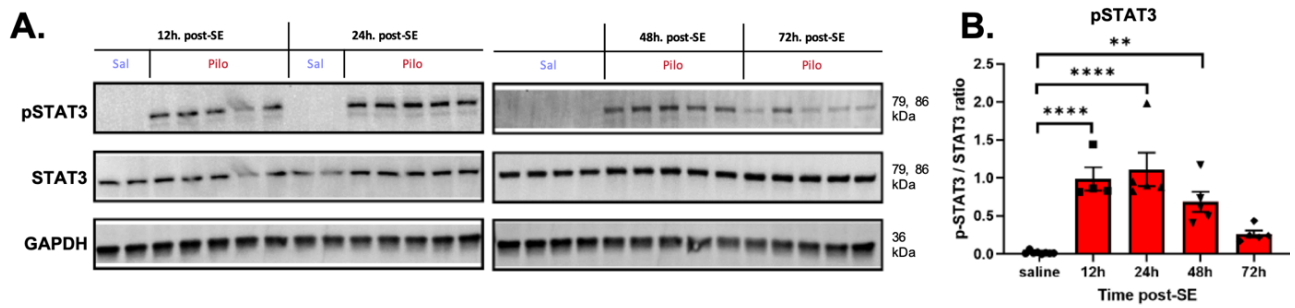

Fig S4. Transient induction of STAT3 in wildtype animals is observed across models of SE. **(A)** Hippocampi were collected from wildtype control and pilo-SE rats at 12, 24, 48, and 72h. post-SE to perform western blotting for pSTAT3, total STAT3, and GAPDH. **(B)** pSTAT3 was induced up to 48h. post-SE, but diminished by 72h. post-SE (1-way ANOVA with Tukey's correction; n=4-8).

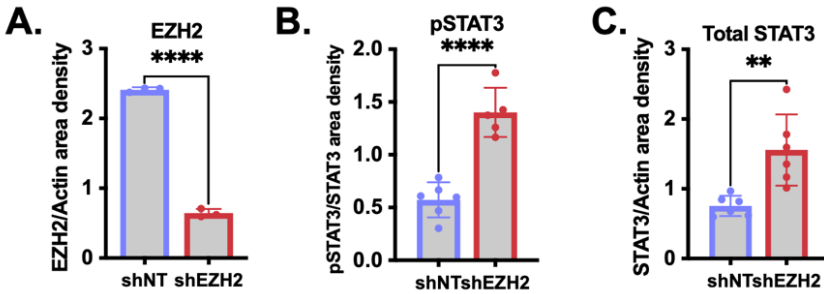

Fig. S5. Western blot quantifications in shNT and shEZH2 N2A cells. Protein was harvested from shNT and shEZH2 cells for western blot analysis. **(A)** EZH2 was reduced 3.7-fold in the knockdown cells (unpaired t-test; n=3). We observed **(B)** a 2.4-fold induction of pSTAT3 (unpaired t-test; n=5-6) and **(C)** a 2.1-fold induction of total STAT3 in shEZH2 cells (unpaired t-test; n=6).

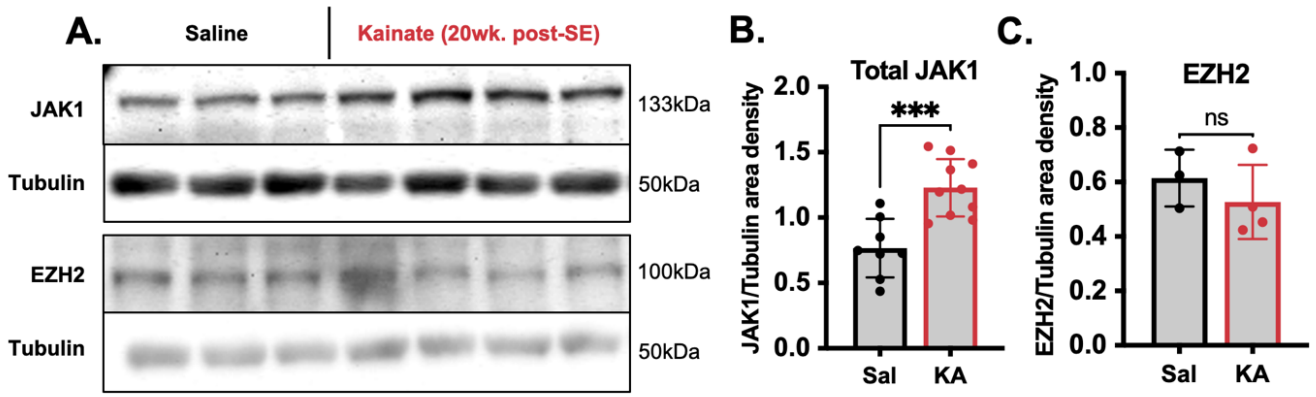

Fig. S6. JAK1 but not EZH2 is induced in chronic epilepsy. **(A)** Hippocampi were harvested from 20wk. post-SE chronically epileptic mice and naïve controls. Protein lysates were subjected to western blotting. **(B)** JAK1 was induced 1.6-fold in chronically epileptic mice compared to naïve (unpaired t-test; p=0.0005), while **(C)** EZH2 was unchanged from naïve levels in chronic epilepsy.

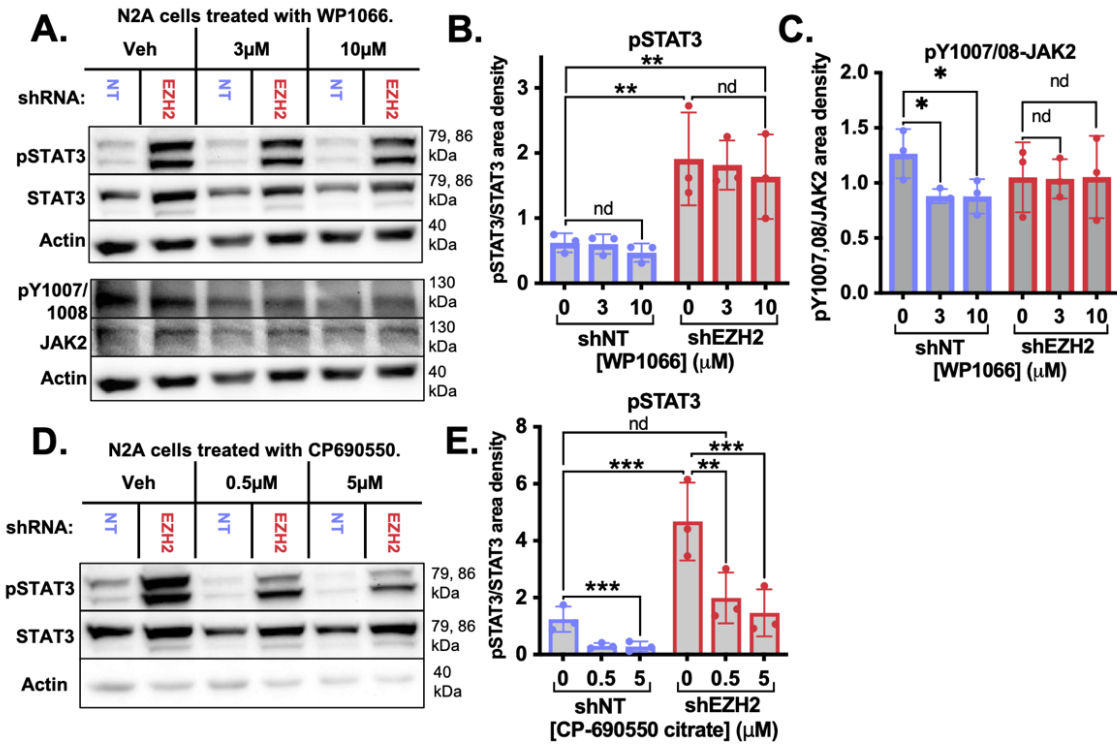

Fig. S7. JAK1/3 but not JAK2 activity is required for hyper-activation of STAT3 in the absence of EZH2. **(A)** shNT and shEZH2 cells were treated with the JAK2/STAT3 inhibitor WP1066 to a final concentration of 0 (DMSO), 3, or 10μM for one hour. **(B)** pSTAT3 was induced in vehicle-treated shEZH2 cells by 3-fold. WP1066 did not alter pSTAT3 levels in control or knockdown cells at any concentration. **(C)** WP1066 reduced pY1007/08-JAK2 in shNT cells for both concentrations. No change was observed in knockdown cells. **(D-E)** pSTAT3 hyperactivation in shEZH2 cells was rescued to shNT levels with the JAK inhibitor CP690550 citrate. pSTAT3 was induced in vehicle-treated shEZH2 cells by 3.7-fold. CP690550 treatment for one hour reduced pSTAT3 levels of KD cells by 2.3-fold at 0.5μM and 3.2-fold at 5μM. At 0.5μM CP, pSTAT3 levels in KD cells were reduced to that of vehicle-treated shNT cells (2-way ANOVA with BKY correction; n=3).

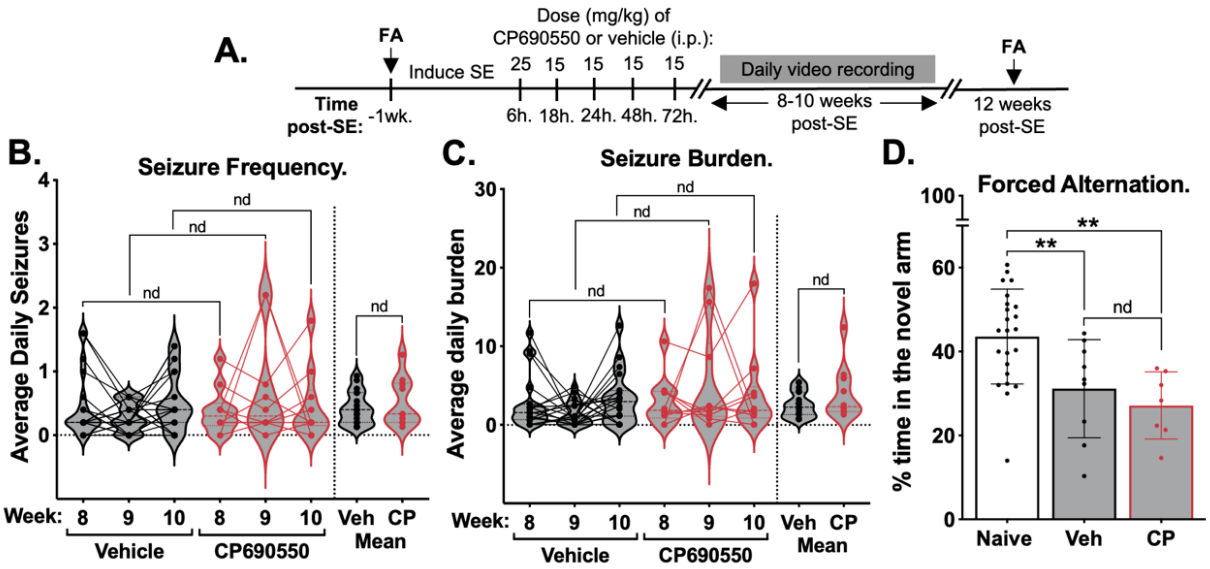

Fig. S8. Transient CP690550 treatment acutely post-SE does not alter epileptogenesis in wildtype mice. **(A)** SE was induced via systemic kainate, and wildtype mice were treated with five doses of either vehicle or CP690550 up to 72h. post-SE. Behavioral spontaneous seizure activity was monitored by video from weeks 8-10 post-SE. Seizure frequency **(B)** and burden scores **(C)** across vehicle- and CP690550-treated mice. Acute treatment with CP690550 was not antiepileptogenic (2-way ANOVA with BKY correction; n=10-20). No week-to-week differences in seizure frequency or burden were detected in vehicle- versus CP690550-treated mice, nor in the average seizure frequency or burden across weeks. **(D)** Short-term memory was assessed by forced alternation Y-maze testing 1 week before SE and 12 weeks post-SE. Acute treatment with CP690550 did not rescue epilepsy-associated memory decline (1-way ANOVA with BKY correction; n=7-23). Chronically epileptic mice showed reduced performance in the forced alternation test regardless of treatment acutely post-SE (**Vehicle:** 29% reduction; **CP690550:** 38% reduction).

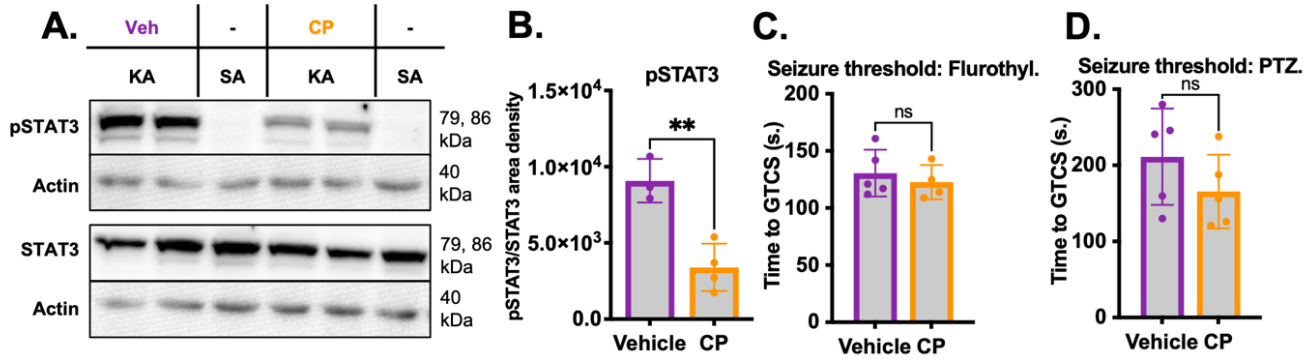

Fig. S9. CP690550 target engagement and threshold testing with pre-treatment. **(A)** After induction of SE and CP treatment at 6, 12, and 24h. post-SE, mice were sacrificed 3 hours after the last injection to confirm drug target engagement via western blot. **(B)** Naïve mice (lanes 3,6) were included to confirm pSTAT3 induction typically observed on day 1 post-SE. Drug-treated animals exhibited a 2.7-fold reduction in pSTAT3 compared to vehicle-treated animals (unpaired t-test; n=3). **(C-D)** To assess the anticonvulsant properties of CP690550, naïve wildtype mice were pre-treated with CP690550 or vehicle (i.p., 15mg/kg) 30 minutes prior to threshold testing with flurothyl or PTZ (i.p., 45mg/kg). Time to generalized tonic clonic seizure was recorded. Results were analyzed by unpaired t-test. CP690550 pre-treatment did not alter **(C)** flurothyl (unpaired t-test; n=4-5) or **(D)** PTZ seizure threshold (unpaired t-test; n=5).

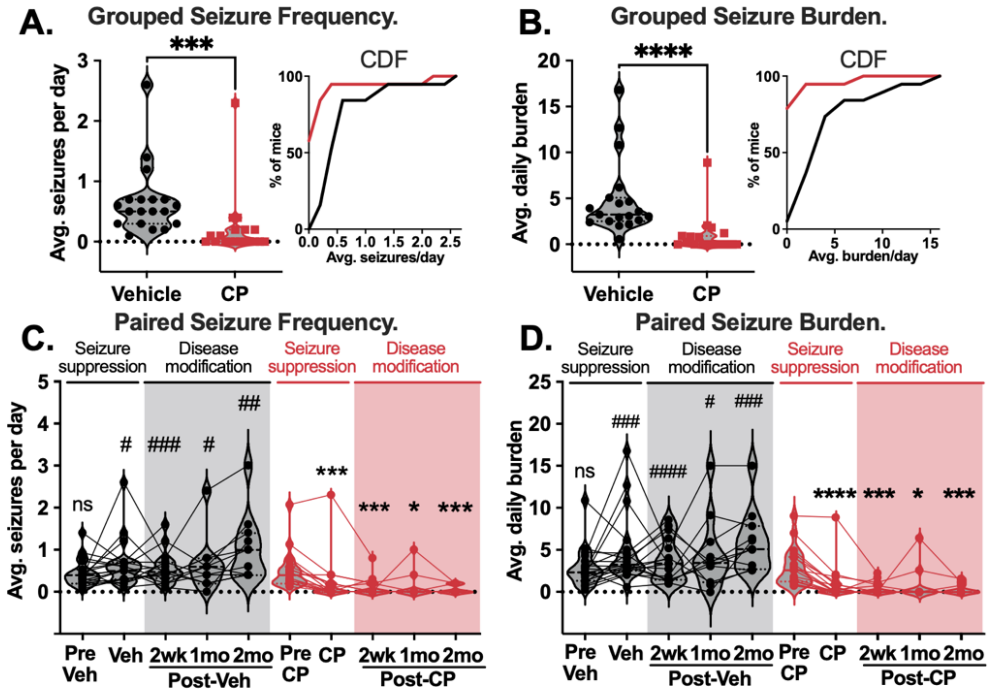

Fig. S10. Long-term SRS data for both responders and non-responders to CP690550 in the systemic kainate model. SE was induced via systemic kainate, and behavioral seizures monitored by video from weeks 8-20 post-SE. Vehicle was administered from weeks 8-10 post-SE, followed by daily vehicle or CP690550 treatment weeks 11-12. After drug washout, video recording continued weeks 13-20 post-SE. **(A-B)** Grouped comparisons for seizure frequency and burden were displayed as violin plots and cumulative frequency distributions (bin centers are marked). Mice treated with CP690550 showed profound reductions in seizure frequency and burden (Kolmogorov-Smirnov test; **Frequency:** 3.2-fold, D:0.68, $p<10^{-3}$, **Burden:** 5.5-fold, D:0.84, $p<10^{-4}$; n=19). Paired seizure frequency **(C)** and burden **(D)** were displayed as violin plots (∗: CP-treated compared to pre-CP, #: vehicle compared to CP-treated) (2-way ANOVA with BKY correction; n=9-19). 2 weeks post-CP690550, mice showed a 5-fold reduction in frequency and 9-fold reduction in burden compared to mice 2 weeks post-vehicle; 10 out of 15 mice (67%) were seizure-free during this time. 2 months after drug washout, treated animals continued to exhibit a 16-fold reduction in seizure frequency and a 15-fold reduction in seizure burden compared to vehicle-treated mice.

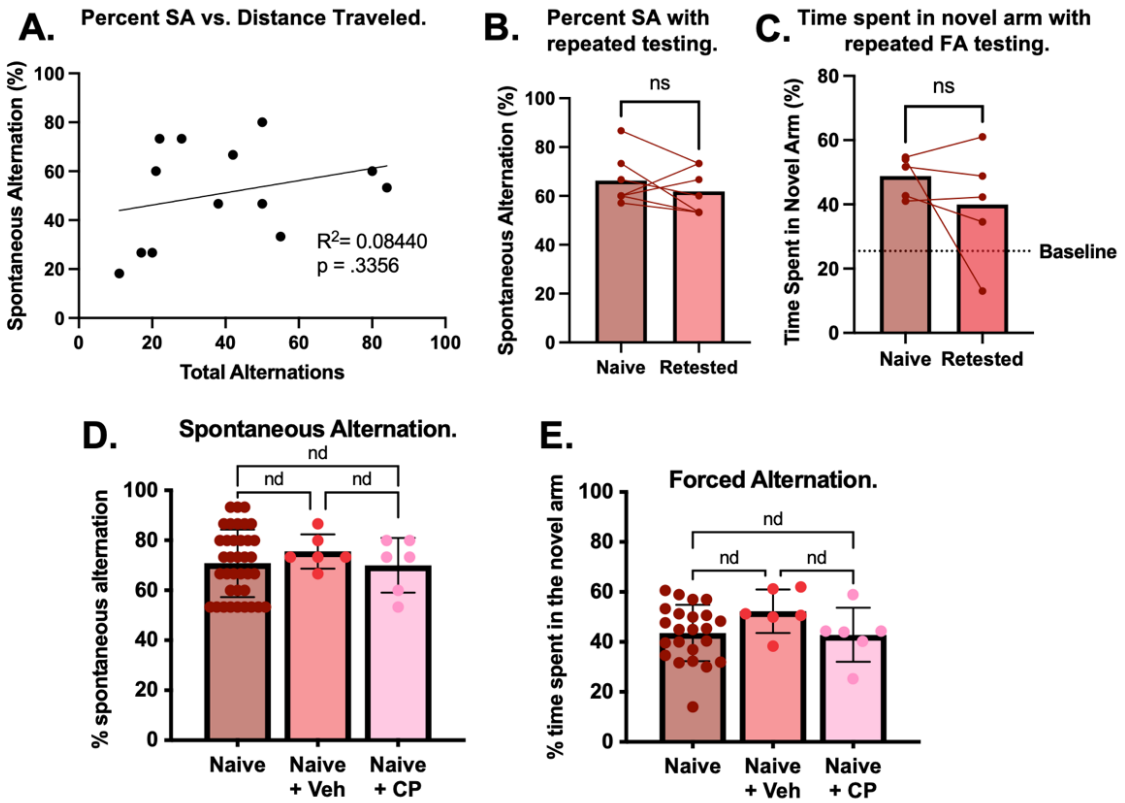

Fig. S11. Distance traveled is not correlated with deficits in spontaneous alternation post-SE, and SA and FA results are not altered with repeated testing or CP690550 treatment in naïve mice. **(A)** Epilepsy-related reductions in working memory (as measured by percent spontaneous alternations) were not correlated to distance traveled as measured by the total number of alternations (Pearson correlation; n=13). Percent spontaneous alternation **(B)** and time spent in the novel arm during the retrieval trial of FA testing **(C)** were not altered by repeated testing (paired t-test; n=5-6). Tests occurred 24 days apart for spontaneous alternation, and 17 days apart for forced alternation. SA **(D)** and FA **(E)** tests were performed on untreated naïve mice, and mice treated with vehicle or CP690550 for two weeks (i.p., 15mg/kg/day). Neither vehicle nor CP treatment altered percent spontaneous alternation or time spent in the novel arm. Panels D-E were analyzed by 1-way ANOVA with BKY's correction for multiple comparisons (**SA:** n=6-37; **FA:** n=6-23).

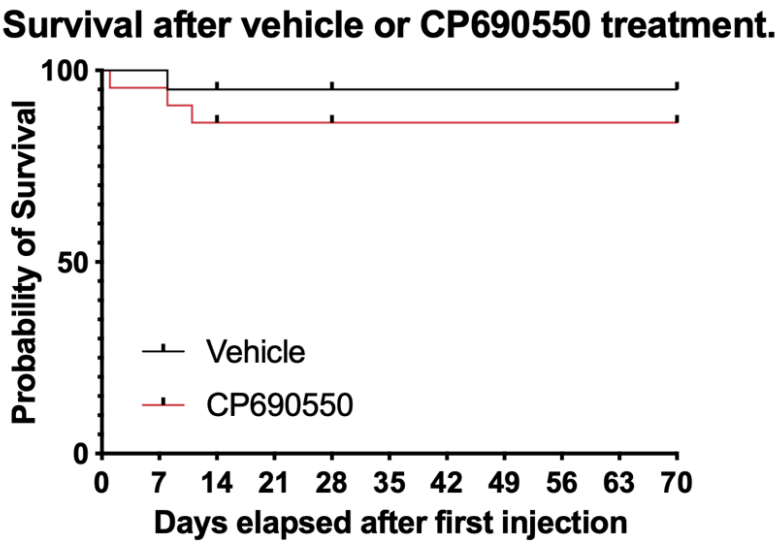

Fig. S12. CP690550 treatment does not increase mortality in chronically epileptic mice. 42 male and female FVB mice were treated with 10 doses of vehicle or CP690550 (15mg/kg/day; i.p.) over two weeks. 38 mice survived treatment. Of the CP690550-treated mice, three died 1, 8, and 11 days after the first day of treatment. Three mice were harvested on the final day of treatment, and six mice were harvested two weeks post-washout. Of the vehicle-treated mice, one died 8 days after the first day of treatment. Four mice were harvested on the final day of treatment, and five mice were harvested two weeks post-washout. There was no difference in survival between treatment groups (Log-rank Mantel-Cox test; Chi square: 0.893, p=0.344).